RESEARCH ARTICLE

American Journal of Botany

Botanical Society of America
leading scientists and educators since 1893

Infraspecific diversification of the star cloak fern (*Notholaena standleyi*) in the deserts of the United States and Mexico

Tzu-Tong Kao[1,4], Carl J. Rothfels[2], Alicia Melgoza-Castillo[3], Kathleen M. Pryer[1], and Michael D. Windham[1]

Manuscript received 20 September 2019; revision accepted 4 February 2020.

[1] Department of Biology, Duke University, Durham, North Carolina 27708, USA

[2] University Herbarium and Department of Integrative Biology, University of California, Berkeley, California 94720, USA

[3] Facultad de Zootecnia y Ecología, Universidad Autónoma de Chihuahua, Chihuahua, Chihuahua CP 31000, Mexico

[4] Author for correspondence (e-mail: tzu.tong.kao@duke.edu)

Citation: Kao, T.-T., C. J. Rothfels, A. Melgoza-Castillo, K. M. Pryer, and M. D. Windham. 2020. Infraspecific diversification of the star cloak fern (*Notholaena standleyi*) in the deserts of the United States and Mexico. *American Journal of Botany* 107(4): 658–675.

doi:10.1002/ajb2.1461

PREMISE: Not all ferns grow in moist and shaded habitats. One well-known example is *Notholaena standleyi*, a species that thrives in deserts of the southwestern United States and Mexico. This species exhibits several "chemotypes" that differ in farina (flavonoid exudates) color and chemistry. By integrating data from molecular phylogenetics, cytology, biochemistry, and biogeography, we circumscribed the major evolutionary lineages within *N. standleyi* and reconstructed their diversification histories.

METHODS: Forty-eight samples were selected from across the geographic distribution of *N. standleyi*. Phylogenetic relationships were inferred using four plastid and five nuclear markers. Ploidy levels were inferred using spore sizes calibrated by chromosome counts, and farina chemistry was compared using thin-layer chromatography.

RESULTS: Four clades are recognized, three of which roughly correspond to previously recognized chemotypes. The diploid clades G and Y are found in the Sonoran and Chihuahuan deserts, respectively; they are estimated to have diverged in the Pleistocene, congruent with the postulated timing of climatological events separating these two deserts. Clade P/YG is tetraploid and partially overlaps the distribution of clade Y in the eastern Chihuahuan Desert. It is apparently confined to limestone, a geologic substrate rarely occupied by members of the other clades. The cryptic (C) clade, a diploid group known only from southern Mexico and highly disjunct from the other three clades, is newly recognized here.

CONCLUSIONS: Our results reveal a complex intraspecific diversification history of *N. standleyi*, traceable to a variety of evolutionary drivers including classic allopatry, parapatry with or without changes in geologic substrate, and sympatric divergence through polyploidization.

KEY WORDS amplicon sequencing; biogeography; cheilanthoids; farina; flavonoids; limestone; missing diploids; phylogenetics; polyploid speciation; Pteridaceae.

Because water is essential for life on Earth, living in deserts is challenging for most organisms. A portion of species, however, have managed to survive, and even diversify, within semi-xeric to xeric environments. One notable example in ferns is the diverse and ecologically unusual cheilanthoid clade (Cheilanthoideae: Pteridaceae), with 20+ genera and 400+ species distributed across the globe (PPG I, 2016). Many cheilanthoids thrive in exposed, seasonally dry environments; one particularly remarkable subgroup of cheilanthoids is the notholaenids, consisting of ~40 species endemic to the deserts of Mexico and the southwestern United States (Rothfels et al., 2008; Kao et al., 2019).

Notholaena standleyi Maxon is one of the most common species of notholaenid ferns. Its distribution is centered in the Sonoran and Chihuahuan deserts, from Baja California in the west to Texas and Coahuila, Mexico, in the east; its northernmost populations are found in Colorado and Oklahoma, and its range extends deep into southern Mexico (Seigler and Wollenweber, 1983; Windham, 1993a; Mickel and Smith, 2004). Recent molecular phylogenies, inferred using both plastid and nuclear sequences, indicate that *N. standleyi* is one of the more isolated lineages within notholaenids (Rothfels et al., 2008; Johnson et al., 2012; Kao et al., 2019), and it is estimated to have diverged from its closest relatives ~55 mya (Testo and Sundue, 2016). Like most other notholaenid ferns, *N. standleyi* has poikilohydric and desiccation-tolerant leaves (Proctor and Pence, 2002; Proctor and

Tuba, 2002; Hietz, 2010), and it produces "farina" (flavonoid exudates) on the abaxial surface of the leaves and on the margins of the gametophyte prothallus (Tryon, 1947; Rothfels et al., 2008; Johnson et al., 2012; Kao et al., 2019).

Farina consists of powdery, lipophilic exudates (composed primarily of flavonoid aglycones) produced by epidermal trichomes (Wollenweber and Schneider, 2000). It evolved in several genera of Pteridaceae, including *Aleuritopteris*, *Argyrochosma*, *Pentagramma*, *Notholaena*, and some other genera with fewer farinose species (Wollenweber and Schneider, 2000). It is hypothesized that farina is an adaptation to drought that reduces water loss from transpiration and/or protects dry, dormant leaves from UV damage (Hevly, 1963; Wollenweber, 1984). Chemotaxonomic studies in cheilanthoid ferns have demonstrated that the farinas of different taxa are often chemically distinct, and these differences occasionally result in distinctive farina colors (reviewed in Wollenweber, 1984; Wollenweber and Schneider, 2000).

Seigler and Wollenweber (1983) identified three such "chemotypes" (infraspecific variants, each with a distinct farina chemistry) within *N. standleyi* and informally recognized them on the basis of farina color: gold (G), yellow (Y), and yellow-green (YG). The farina of chemotype G consisted mostly of 7-O-methylkaempferol and 4′-O-methylkaempfer, whereas the farina of chemotype Y consisted mostly of kaempferol, 3-O-methylkaempferol and 4′-O-methylkaempferol; the farina of chemotype YG appeared to combine major compounds from G and Y, but its most abundant component was usually 4′-O-methylkaempfer. Seigler and Wollenweber (1983) further noted that these differences in farina chemistry showed correlations with both geographic distribution and substrate preferences. According to their data, chemotype G was largely confined to the Sonoran Desert, chemotype Y occupied a broad territory extending from Colorado (USA) to Oaxaca (Mexico), and chemotype YG was concentrated in the eastern Chihuahuan Desert. Seigler and Wollenweber (1983) also reported that chemotypes G and Y preferred igneous rocks, whereas YG was restricted to limestone.

In the mid-1990s, one of us (Windham) noted the existence of another potential chemotype, confined to limestone outcrops in southeastern Arizona. This chemotype, tentatively referred to as "pallid" (P), had light-colored farina resembling that of chemotype Y, but its spores were significantly larger, suggesting the possibility of polyploidy. Previously published chromosome counts for *N. standleyi* (obtained from populations of both the Y and G chemotypes) were all diploid ($n = 30$ or $2n = 60$; see Knobloch et al., 1973; Smith, 1974; Windham and Schaack, 1983; Benham, 1988). The chromosome number of chemotype YG had not been determined, but it produced large spores similar to those of the "pallid" (P) populations. Recent cytogenetic work on "pallid" has shown that it is indeed tetraploid ($n = 60$; Kao et al., 2019).

Notholaena standleyi provides a unique opportunity to study the evolution of infraspecific diversity among xeric-adapted ferns. The taxon is widespread and variable but, in deference to its apparent morphological uniformity, no author in the past century has attempted to split it nomenclaturally. Yet we now know that it comprises at least four farina chemotypes that differ in geographic distribution, substrate preferences, and ploidy. To capture a broader picture of the diversification patterns within *N. standleyi*, we studied collections from recent fieldwork and several major herbaria in the United States and Mexico. A total of 48 specimens encompassing the geographic breadth of each of the recognized chemotypes of *N. standleyi* was selected for in-depth analyses of molecular phylogeny, cytology, and farina biochemistry. On the basis of these data, we infer the infraspecific phylogeny of *N. standleyi*, circumscribe the major evolutionary lineages within the species, and discuss factors that may have contributed to its diversification in arid regions of the southwestern United States and Mexico.

MATERIALS AND METHODS

Taxon sampling

To screen for molecular variation within *N. standleyi*, DNA was extracted from a total of 76 samples, spanning most of the geographic distribution of the species, and the plastid intergenic spacer *trnG-trnR* was amplified and sequenced. The *trnG-trnR* phylogeny was inferred using 82 *N. standleyi* samples (including six samples published in Rothfels et al., 2008 and Kao et al., 2019) and 14 outgroups representing the major lineages of cheilanthoid ferns (notholaenids, hemionitids, pellaeids, and myriopterids). A full list of molecular voucher specimens is provided in Appendix 1. On the basis of this initial study, 48 *N. standleyi* samples were selected for further molecular, cytological, and biochemical analyses.

DNA isolation, amplification, sequencing

Genomic DNA was isolated from silica-dried or air-dried herbarium material using the E.Z.N.A. SP Plant DNA Kit (Omega, Norcross, Georgia, USA), following modifications described in Schuettpelz and Pryer (2007). Four plastid markers and five nuclear markers were amplified and sequenced. Among the three plastid markers used by Kao et al. (2019) for reconstructing the phylogeny of notholaenids, only the intergenic spacer *trnG-trnR* was included in this study because the other two plastid markers, *rbcL* and *aptA*, evolve too slowly to be useful in resolving an infraspecific phylogeny. The plastid data set also included two additional intergenic spacers (*trnL-trnF* and *matK-rps16*) and one fast-evolving gene (*ndhF*; see Wei et al., 2017); most of the primers were newly designed here to amplify taxa from the notholaenid and hemionitid subclades (Table 1). All five nuclear markers analyzed here are intron-spanning and were selected from the list of single-/low-copy genes recommended by Rothfels et al. (2013). Four of the five (*ApPEFP_C*, *gapCpSh*, *IBR3*, and *SQD1*) were used in Kao et al. (2019); *transducin* was newly added here. The primers for *IBR3* and *SQD1* were newly designed here to be able to amplify longer regions. All primers used in this study are summarized in Table 1; some were published in Nagalingum et al. (2007), Li et al. (2010), Sigel et al. (2011), Rothfels et al. (2013), and Kao et al. (2019); all others were newly designed for this study. The new plastid primers (for *matK–rps16* and *ndhF*) were designed using an alignment of six chloroplast genomes of cheilanthoids (*Cheilanthes micropteris* Sw.: MH173078; *Hemionitis subcordata* [D.C. Eaton ex Davenp.] Mickel: MH173072; *Myriopteris covillei* [Maxon] Á. Löve & D. Löve: MG953517; *M. lindheimeri* [Hook.] J. Sm.: HM778032; *N. standleyi*: MH173067; and *Pentagramma triangularis* [Kaulf.] Yatsk., Windham & E. Wollenw.: MH173070). The new nuclear primers (*IBR3*, *SQD1*, and *transducin*) were designed using transcriptome-based alignments from Rothfels et al. (2013), and the intron lengths of *IBR3* and *SQD1* were predicted using the *N. standleyi* sequences published in Kao et al. (2019).

Polymerase chain reaction (PCR) amplifications were carried out in 25 μL reactions that included 1 μL DNA template,

TABLE 1. Primers used in this study.

Locus	Amplification length	Primer	Direction	Utility	Sequence (5′–3′)	Reference
trnG-trnR	~1160 bp	TRNG1F	Forward	Amplification, sequencing	GCGGGTATAGTTTAGTGGTAA	Nagalingum et al., 2007
		TRNG63R	Reverse	Sequencing	GCGGGAATCGAACCCGCATCA	Nagalingum et al., 2007
		TRNGJBF	Forward	Sequencing	AGGAGCCGAATGGGCCGAAA	Sigel et al., 2011
		TRNR22R	Reverse	Amplification, sequencing	CTATCCATTAGACGATGGACG	Nagalingum et al., 2007
matK-rps16	~899 bp	matK-7F	Forward	Amplification, barcoded	AACTCCCAAACAAGCATTGG	This study
		rps16_869R	Reverse	Amplification	ATCTCGATAAATGACTTACCGA	This study
ndhF	994 bp	NDHF90F	Forward	Amplification, barcoded	TCCGTAACGTATACCYTCCCC	This study
		NDHF1126R	Reverse	Amplification	AGCCGGTTCAGTAATTCACTC	This study
trnL-trnF	~916 bp	FernL 1Ir1	Forward	Amplification, barcoded	GGYAATCCTGAGCCAAATC	Li et al., 2010
		TRNFF_Noth	Reverse	Amplification	AWTTGAACTGGTGACACGAG	This study
ApPEFP_C	~975 bp	APPNOTHF	Forward	Amplification, barcoded	GCAGGRCCYGGCCTTGCTGAGGA	Kao et al., 2019
		APPNOTHR	Reverse	Amplification	GCAACATGAGCRGCTGGTTCACGRGG	Kao et al., 2019
gapCpSh	~829 bp	NOTHGAPF	Forward	Amplification	GAGGRTKCTTAYAAACCAGAGATGC	Kao et al., 2019
		NOTHGAPR	Reverse	Amplification, barcoded	CTTCAGTATAACCCAAAATTCC	Kao et al., 2019
IBR3	~1074 bp	IBRNOTHF	Forward	Amplification	AAAGAAAGTGGCTCARGCCT	This study
		IBRNOTHR	Reverse	Amplification, barcoded	TTAGCGGCATTCAGTACAAGC	This study
SQD1	~930 bp	SQDNOTHF2	Forward	Amplification	AAGGCCTGGAAAATYAGAGC	This study
	~751 bp	SQDNOTHF	Forward	Amplification	CATCCTCTTACAGTYTAYGGHAAAGG	Kao et al., 2019
		SQDNOTHR	Reverse	Amplification, barcoded	CYCTGATRTCAAGGTATCCTCTTGT	Kao et al., 2019
transducin	~768 bp	TRANOTHF	Forward	Amplification, barcoded	ATGGTCACAAGCTACCTGTGC	This study
	~539 bp	6928_3406R_Noth	Reverse	Amplification	CGCTCCCATCTTCGAATRGA	Rothfels et al., 2013
		6928_3802R_Noth	Reverse	Amplification	GTCASAGATTCTTGRGTTTG	Rothfels et al., 2013

2.5 µL Denville 10x PCR buffer containing 15mM $MgCI_2$ (Thomas Scientific, Swedesboro, New Jersey, USA), 2.5 µL 2 mM dNTPs, 1.25 µL forward primer, 1.25 µL reverse primer, 0.25 µL bovine serum albumin (10 mg/mL), 0.25 µL Denville Choice Taq (5 U/µL; Thomas Scientific), and nuclease-free water. The thermocycling conditions comprised an initial denaturation at 94°C for 180 s, 45 cycles at 94°C for 60 s, an annealing temperature (see below) for 90 s, and 72°C for 90 s, with a final extension at 72°C for 600 s. The annealing temperatures for *ndhF*, *matK-rps16*, *trnG-trnR*, *trnL-trnF*, *ApPEFP_C*, *gapCpSh*, *IBR3*, *SQD1*, and *transducin* were 58°C, 55°C, 50°C, 55°C, 68°C, 56°C, 58°C, 58°C, and 58°C, respectively. PCR products from the plastid marker *trnG-trnR* were cleaned using an ExoSAP-IT PCR cleanup kit (United States Biochemical, Cleveland, Ohio, USA) following Schuettpelz et al. (2015), and were sequenced using the PlateSeq Service provided by Eurofins Genomics (Louisville, Kentucky, USA) on a 3730XL DNA Analyzer (Applied Biosystems, Waltham, Massachusetts, USA) using Big Dye Terminator version 3.1 Cycle Sequencing reagents. The reads were assembled using SeqMan Pro (DNASTAR, 2019). The other eight markers were sequenced on the PacBio Sequel platform (Rhoads and Au, 2015) at the Duke Center for Genomic and Computational Biology (https://genome.duke.edu). The target sequences for each sample were amplified separately using barcoded primer sets, whereby either the forward or reverse primer (see Table 1) included a 16-base barcode that was designed for demultiplexing on the Sequel system (PacBio PN 101-629-100, https://www.pacb.com/wp-content/uploads/Sequel_RSII_96_barcodes_v1.fasta.zip). Some individual barcodes were used twice, for one *N. standleyi* and one outgroup taxon. These were later distinguished phylogenetically within the PURC bioinformatics pipeline (Rothfels et al., 2017). The amplified products were visualized on a 1% agarose gel at 80 V for 60 min to confirm amplification success and to allow samples to be pooled in approximately equal concentrations. Bands were scored by eye and sorted into five band-strength categories from "very strong" to "very weak"; a base volume of 0.5 µL, 1 µL, 2 µL, 4 µL, and 8 µL was assigned to each sample that fell within each of these five categories, respectively. Aliquots of the "base volume" times the expected copy number (plastid markers = 1; nuclear markers of diploids = 2; nuclear markers of tetraploids = 4) were taken from each sample and pooled together. From the pooled sample, an aliquot of 150 µL was extracted, cleaned with 1X AMPure XP beads (Beckman Coulter, Brea, California, USA), and sequenced in a single PacBio Single Molecule Real-Time (SMRT) cell utilizing PacBio's (Menlo Park, California, USA) circular consensus sequencing (CCS) technology (Travers et al., 2010). The raw CCS reads were cleaned using USEARCH version 7.0.1090 (Edgar, 2010) to remove any sequences that were <500 bp or had >5 expected errors. The cleaned reads were then demultiplexed and clustered using PURC (Rothfels et al., 2017). Clusters with fewer than four reads were removed. The final set of sequences was selected from the clustering results of eight different PURC regimes (four sets of clustering thresholds: "0.997, 0.995, 0.990, 0.997"; "0.997, 0.997, 0.995, 0.995"; "0.995, 0.995, 0.995, 0.995"; or "0.995, 0.995, 0.990, 0.990"; and two UCHIME abskew settings: 1.9 or 1.1), following the methods described by Rothfels et al. (2017) and Kao et al. (2019).

Sequence alignment and phylogenetic analyses

The DNA data sets of the nine molecular makers were aligned separately using MUSCLE (Edgar, 2004) in ALIVIEW version 1.19 (Larsson, 2014). Besides the newly obtained sequences, six other *N. standleyi* sequences published in Rothfels et al. (2008) and Kao et al. (2019) were added to the alignment. Because our focus was on the infraspecific phylogeny of *N. standleyi*, all samples within

the species were aligned first, and then the outgroups were added and aligned to the existing *N. standleyi* alignment using MUSCLE in ALIVIEW. Preliminary maximum parsimony bootstrap analyses were carried out in PAUP* version 4.0a (Swofford, 2003). Because there were no topological conflicts for the significantly supported clades (MLBS ≥70%) among the four plastid markers, these data sets were concatenated into one "plastid" data set.

Prior to model selection, each data set was partitioned by coding/noncoding and codon position, and a neighbor-joining tree was inferred using PAUP*. The optimal partitioning strategy, and the best model for each data subset—selected among six exchangeability components (JC, F81, K80, HKY, SYM, and GTR) and four among-site rate variation models (equal, +I, +G, and +I+G)—were then selected on the basis of the Bayesian information criterion, using the "automated partitioning" tool implemented in PAUP*. The best-fitting models/partitions for each data set are provided in Appendix S1.

Maximum likelihood (ML) analyses were carried out using Garli version 2.0 (Zwickl, 2006). The best ML tree was selected from among four replicates, each from a different random-addition-sequence starting tree, with genthreshfortopoterm set to 1 million. ML bootstrap support (MLBS) was calculated from 1000 replicates, with genthreshfortopoterm set to 20,000. The Bayesian analyses were carried out in MrBayes version 3.2.3 (Ronquist et al., 2012), with two independent Markov chain Monte Carlo (MCMC) runs, each with four chains, run for 1 million generations. Trees and parameters were sampled every 1000 generations. The mixing and convergence of parameters was inspected using Tracer version 1.6 (Rambaut et al., 2018), and the first 25% of each chain was discarded as burn-in. The resulting phylogenetic trees were rooted using a representative from the myriopterid clade (*Myriopteris aurea* [Poir.] Grusz & Windham) and one from the pellaeid clade (*Paragymnopteris marantae* [L.] K.H. Shing) based on the relationships recovered by Rothfels et al. (2008).

Lineage divergence times for the plastid data set were estimated using BEAST version 2 (Bouckaert et al., 2013). A lognormal relaxed clock model and a birth-death tree model were used. Because there are no appropriate fossils that directly apply, three nodes (circled 1–3 in Fig. 3) were secondarily calibrated using divergence times estimated by Testo and Sundue (2016: supplementary data 2). Normal distribution priors that use their height median as the mean and the sigma were adjusted so that the range between 2.5 percentile and 97.5 percentile fully covered their 95% highest posterior density (HPD). Two independent MCMC runs with 100 million generations were carried out. The convergence of parameters was inspected using Tracer. Trees were sampled every 10,000 generations, and the first 25% of trees were discarded as burn-in. The maximum clade credibility tree was summarized using TreeAnnotator in BEAST.

Assessing ploidy

The ploidy of individuals included in the phylogenetic analyses was inferred by measuring spores and comparing these to spore samples from plants whose ploidy level was established by direct counting of chromosomes. This approach is based on the well-established correlation between spore size and ploidy level within cheilanthoid ferns (Grusz et al., 2009; Beck et al., 2010; Schuettpelz et al., 2015; Kao et al., 2019). Four of the plants providing DNA samples had chromosome counts: T.-T.Kao 17-004 (n = 30), T.-T. Kao 17-010 (n = 60), T.-T.Kao 17-016 (n = 30), and M.D.Windham 525 (n = 30). The first three counts were published in Kao et al. (2019), and the fourth is newly published here. The latter was obtained from meiotic material gathered from a greenhouse-grown plant following the protocols of Windham and Yatskievych (2003).

Among the 48 samples included in the focused phylogenetic analyses, 41 yielded the mature, unopened sporangia required for spore counting and measurement. A few (one to three) such sporangia were removed using dissecting needles, transferred to individual droplets of glycerol on a glass microscope slide. These were carefully opened with the needles under a Leica MZ 7.5 stereomicroscope (Leica Microsystems, Buffalo Grove, Illinois, USA) to release the spores. After removing sporangial debris, the number of spores per sporangium was determined. The spores were then left overnight so that they gathered at the top surface of the glycerol drop, which facilitated measuring spore diameters using a compound REVOLVE (Echo, San Diego, California, USA) microscope. The mean, median, first quartile, third quartile, and standard deviation of measurements from 25 spores were calculated for each sampled individual. The ploidy of these specimens was then inferred by comparison to samples with chromosome counts.

Biochemical comparisons

The farina biochemistry of individual samples included in the phylogenetic analyses was compared using thin layer chromatography (TLC). Sixteen reference samples representing Seigler and Wollenweber's (1983) gold (G), yellow (Y), typical yellow-green (YG), and "anomalous" yellow-green (YG?) chemotypes were used as standards. Farina from each sample was removed from an approximately 0.5 × 0.5 cm^2 leaf segment by rinsing the abaxial surface with acetone. Extracts were collected in small glass sample tubes and concentrated in a fume hood. The TLC analyses were carried out on glass plates that were coated with silica gel matrix, using the solvent system toluene:dioxane:MeOH = 80:10:10 (solvent B in Seigler and Wollenweber, 1983). On each plate, four of the reference samples that represent G, Y, YG, and YG? (one each) were run in the center four columns as a standard. Chromatograms were visualized under both longwave (366 nm) and shortwave (254 nm) UV light. Ten different chemicals were recognized on the TLC plates, and their strengths were ranked on a scale of 0–4 for each sample. Spraying the plates with 2-aminoethyl diphenylborinate, following Seigler and Wollenweber (1983), only enhanced the color of a few compounds under visible light. Because all of these compounds were clearly visible under UV light, data derived from this extra step were not used in the quantitative analyses. Following Seigler and Wollenweber (1983), we did a principal component analysis (PCA) on our TLC data. To optimize the utility of our analyses for classification, we also did a linear discriminant analysis (LDA), by which the samples were assigned to groups C, G, P, Y, or YG, based on our molecular phylogenetic results. Both PCA and LDA analyses were carried out in R (R Development Core Team, 2008).

RESULTS

Plastid phylogeny

The exploratory *trnG-trnR* data set of 96 cheilanthoid ferns resulted in a generally well-supported phylogeny. The maximum likelihood

tree (Fig. 1A) shows a fully supported monophyletic group comprising the hemionitid and notholaenid clades, both of which also receive maximum support. Within the notholaenid clade, the 82 samples of *N. standleyi* form a fully supported monophyletic group whose relationships to other notholaenid groups remain poorly resolved. Within *N. standleyi*, all samples of the P and YG chemotypes form a strongly supported clade, as do the three individuals from southern Mexico herein referred to as the cryptic (C) chemotype. These are well separated from the other known chemotypes by a strict association with limestone substrates (P/YG) or strong geographic isolation (chemotype C; Fig. 1B). By contrast, neither the G nor Y chemotypes receive statistical support in this analysis (Fig. 1A).

Based on the *trnG-trnR* phylogeny and the geographic ranges of the various chemotypes, 48 samples were selected for further molecular, cytological, and biochemical analyses. These samples were arbitrarily assigned numbers between 1 and 48, which appear in parentheses following the sample designators in the *trnG-trnR* phylogeny (Fig. 1A). Table 2 provides a list of these samples along with their voucher data, and Figure 2 presents the phylogeny inferred for this data set based on the four concatenated plastid markers. The latter results are fully congruent with the *trnG-trnR* phylogeny (Fig. 1A) but the resolution is significantly enhanced. Plastid sequences of the yellow-green (YG) and pallid (P) chemotypes are essentially identical, and the fully supported clade formed by these two chemotypes (P/YG in Fig. 2) is sister to a strongly supported clade containing all other *N. standleyi* samples. Within this sister clade to P/YG, the three samples representing the southern Mexican cryptic (C) group form a fully supported monophyletic group sister to populations from northern Mexico and the southwestern United States. The most significant difference between the *trnG-trnR* tree (Fig. 1A) and the concatenated plastid data set (Fig. 2) involves support for and resolution among the northern samples of *N. standleyi*. In contrast to the *trnG-trnR* tree, this group is well supported and is further subdivided into two well-supported clades representing the gold (G) and yellow (Y) chemotypes, respectively.

Diversification times among the major clades of *N. standleyi* were inferred on the basis of the plastid data set and three secondarily calibrated nodes (labeled 1–3 in Fig. 3). Compared to the time of divergence of *N. standleyi* from other notholaenids (~55 mya), divergence times among the infraspecific clades are relatively recent (<10 mya; Fig. 3). The mean estimated divergence times between the clades P/YG and C + G + Y, the clades C and G + Y, and the clades Y and G are 6.4 mya (95% HPD 3.7–9.3 mya), 3.2 mya (95% HPD 1.9–4.6 mya), and 2.1 mya (95% HPD 1.3–3.1 mya), respectively.

Nuclear phylogeny

The five single-locus nuclear phylogenies (*ApPEFP_C*, *gapCpSh*, *IBR3*, *SQD1*, and *transducin*) are presented in Figure 4. The clades identified by the plastid phylogeny are highlighted here with matching color blocks, and an abbreviated name for each clade/grade is provided near the base of each. These classification results are also summarized in Table 2. All P and YG samples amplified for *ApPEFP_C*, *SQD1*, and *transducin* showed two alleles (designated a and b), providing evidence of widespread gene duplication in these chemotypes. In *ApPEFP_C* and *SQD1*, the "a" allele falls in a strongly supported clade that appears to be sister to all other samples, whereas the "b" allele (also monophyletic) appears to be more closely related to the G and Y chemotypes. At the *transducin* locus, the well-supported "a" allele clade of P and YG appears to be sister to the G clade, with these two combined potentially sister to all remaining samples. This is the only marker in the study clearly separating the P and YG chemotypes; in this case, the "b" alleles derived from P and YG form distinct clades (Fig. 4E). The *gapCpSh* tree presents a slight variation on this theme, with the "a" alleles strongly supported as sister to all other samples of *N. standleyi* and the "b" alleles found in two clades, one consisting solely of YG samples and the other composed almost exclusively of P (Fig. 4B). Amplification of *gapCpSh* was somewhat less consistent; we retrieved only one copy of the gene from three of the P/YG samples (nos. 15, 44, and 46). On the *IBR3* tree, the majority of P/YG samples exhibited a single allele (Fig. 4C). The only two exceptions (nos. 15 and 42) were sequenced by Kao et al. (2019) using a different set of primers that amplify a shorter region.

The three samples of chemotype C form a monophyletic group in the *ApPEFP_C*, *gapCpSh*, and *SQD1* trees (Fig. 4A, B, D) but appear to be paraphyletic in the *transducin* tree (Fig. 4E). Placement of this clade in the tree in relation to other groups is variable; only in the case of *ApPEFP_C* does the topology approximate the well-supported concatenated plastid phylogeny (Fig. 2). The sequences of the two samples from Oaxaca (derived from the same population) are nearly identical at all loci analyzed. We failed to amplify and sequence the *IBR3* marker from the three clade C samples, using either the new primer set designed for this study (Table 1) or the primers published in Kao et al. (2019).

Samples of chemotype G form a well-supported clade in the *ApPEFP_C*, *gapCpSh*, and *transducin* trees (Fig. 4A, B, E), with the exception of one rogue *transducin* copy obtained from sample no. 11. Chemotype G is paraphyletic in the *IBR3* and *SQD1* trees (Fig. 4C, D) and shows appreciable levels of heterozygosity in all markers except *gapCpSh*. In the case of the *ApPEFP_C* locus, half of the individuals amplified were heterozygous and the alleles formed two well-supported clades strongly resolved as sister to one another (Fig. 4A). Nuclear sequence data indicate that chemotype Y is potentially monophyletic (though lacking statistical support) in the *transducin* tree (Fig. 4E). On the basis of all other markers, it is paraphyletic or unresolved in relation to one or more of the other *N. standleyi* clades. Allelic diversity is somewhat higher than that observed in chemotype G, some of this diversity is clustered in discernible clades, and heterozygosity (which is almost as prevalent as in chemotype G) often bridges these groups (Fig. 4). In the *gapCpSh* and *IBR3* trees (Fig. 4B, C), the "b" alleles of P/YG samples are nested within the Y clades/grades, suggesting that the Y chemotype may be part parental to the P/YG lineage.

Geography and geologic substrate

Chemotype P is apparently rare, known only from southeastern Arizona and northern Sonora (Fig. 1B). The distribution of chemotype YG is concentrated in Coahuila, Mexico, but it occurs throughout much of the eastern Chihuahuan Desert, including southern Texas, Zacatecas, Durango, and Chihuahua. In this study, we document a new record for this chemotype in Otero County, New Mexico (Fig. 1B), a northwestward extension of its known range by >400 km.

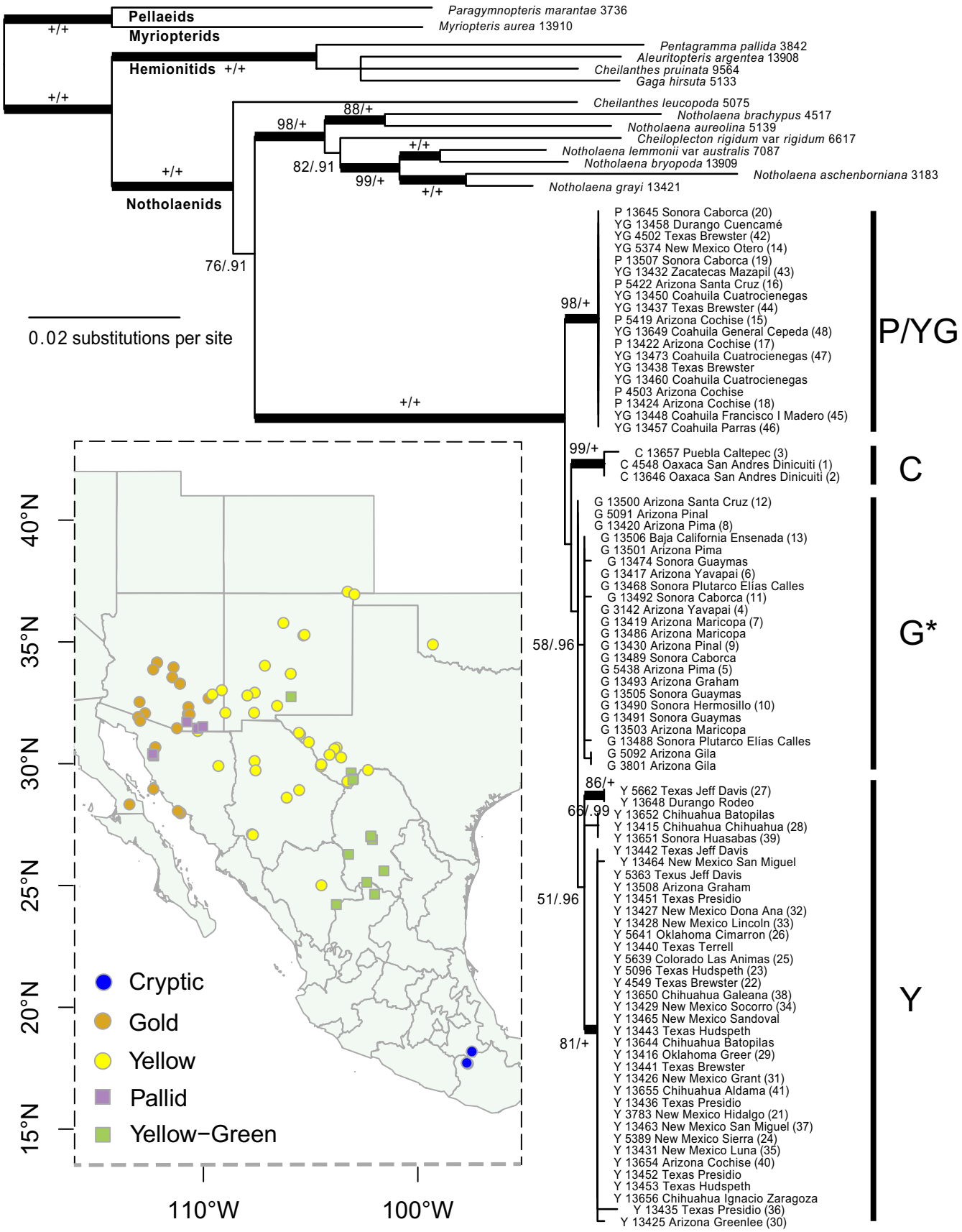
Pellaeids
Myriopterids
Hemionitids
Notholaenids
Paragymnopteris marantae 3736
Myriopteris aurea 13910
Pentagramma pallida 3842
Aleuritopteris argentea 13908
Cheilanthes pruinata 9564
Gaga hirsuta 5133
Cheilanthes leucopoda 5075
Notholaena brachypus 4517
Notholaena aureolina 5139
Cheiloplecton rigidum var rigidum 6617
Notholaena lemmonii var australis 7087
Notholaena bryopoda 13909
Notholaena aschenborniana 3183
Notholaena grayi 13421
0.02 substitutions per site
P 13645 Sonora Caborca (20)
YG 13458 Durango Cuencamé
YG 4502 Texas Brewster (42)
YG 5374 New Mexico Otero (14)
P 13507 Sonora Caborca (19)
YG 13432 Zacatecas Mazapil (43)
P 5422 Arizona Santa Cruz (16)
YG 13450 Coahuila Cuatrocienegas
YG 13437 Texas Brewster (44)
P 5419 Arizona Cochise (15)
YG 13649 Coahuila General Cepeda (48)
P 13422 Arizona Cochise (17)
YG 13473 Coahuila Cuatrocienegas (47)
YG 13438 Texas Brewster
YG 13460 Coahuila Cuatrocienegas
P 4503 Arizona Cochise
P 13424 Arizona Cochise (18)
YG 13448 Coahuila Francisco I Madero (45)
YG 13457 Coahuila Parras (46)
P/YG
C 13657 Puebla Caltepec (3)
C 4548 Oaxaca San Andres Dinicuiti (1)
C 13646 Oaxaca San Andres Dinicuiti (2)
C
G 13500 Arizona Santa Cruz (12)
G 5091 Arizona Pinal
G 13420 Arizona Pima (8)
G 13506 Baja California Ensenada (13)
G 13501 Arizona Pima
G 13474 Sonora Guaymas
G 13417 Arizona Yavapai (6)
G 13468 Sonora Plutarco Elías Calles
G 13492 Sonora Caborca (11)
G 3142 Arizona Yavapai (4)
G 13419 Arizona Maricopa (7)
G 13486 Arizona Maricopa
G 13430 Arizona Pinal (9)
G 13489 Sonora Caborca
G 5438 Arizona Pima (5)
G 13493 Arizona Graham
G 13505 Sonora Guaymas
G 13490 Sonora Hermosillo (10)
G 13491 Sonora Guaymas
G 13503 Arizona Maricopa
G 13488 Sonora Plutarco Elías Calles
G 5092 Arizona Gila
G 3801 Arizona Gila
G*
Y 5662 Texas Jeff Davis (27)
Y 13648 Durango Rodeo
Y 13652 Chihuahua Batopilas
Y 13415 Chihuahua Chihuahua (28)
Y 13651 Sonora Huasabas (39)
Y 13442 Texas Jeff Davis
Y 13464 New Mexico San Miguel
Y 5363 Texus Jeff Davis
Y 13508 Arizona Graham
Y 13451 Texas Presidio
Y 13427 New Mexico Dona Ana (32)
Y 13428 New Mexico Lincoln (33)
Y 5641 Oklahoma Cimarron (26)
Y 13440 Texas Terrell
Y 5639 Colorado Las Animas (25)
Y 5096 Texas Hudspeth (23)
Y 4549 Texas Brewster (22)
Y 13650 Chihuahua Galeana (38)
Y 13429 New Mexico Socorro (34)
Y 13465 New Mexico Sandoval
Y 13443 Texas Hudspeth
Y 13644 Chihuahua Batopilas
Y 13416 Oklahoma Greer (29)
Y 13441 Texas Brewster
Y 13426 New Mexico Grant (31)
Y 13655 Chihuahua Aldama (41)
Y 13436 Texas Presidio
Y 3783 New Mexico Hidalgo (21)
Y 13463 New Mexico San Miguel (37)
Y 5389 New Mexico Sierra (24)
Y 13431 New Mexico Luna (35)
Y 13654 Arizona Cochise (40)
Y 13452 Texas Presidio
Y 13453 Texas Hudspeth
Y 13656 Chihuahua Ignacio Zaragoza
Y 13435 Texas Presidio (36)
Y 13425 Arizona Greenlee (30)
Y
88/+
98/+
82/.91
99/+
76/.91
98/+
99/+
58/.96
86/+
66/.99
51/.96
81/+
+/+
40°N
35°N
30°N
25°N
20°N
15°N
110°W
100°W
Cryptic
Gold
Yellow
Pallid
Yellow−Green

FIGURE 1. Distribution of samples belonging to the five chemotypes (four clades) of *Notholaena standleyi* and their phylogenetic relationships inferred using plastid intergenic spacer *trnG-trnR*. The best maximum likelihood (ML) tree is presented. Branches with ≥70% ML bootstrap support and ≥0.95 posterior probability (PP) are thickened and their support values (ML bootstrap/PP) are shown on the branches. The plus signs indicate that the ML bootstrap = 100% or PP = 1. Forty-eight samples were selected from this phylogeny for further molecular, cytological, and biochemistry analyses. These selected samples are numbered in a series from 1 to 48 (Table 2), which are shown in parentheses after the sample names. The chemotypes are summarized at the right side of the ML tree (C = cryptic, G = gold, P = pallid, Y = yellow, YG = yellow-green). Although the gold chemotype is paraphyletic on this *trnG-trnR* tree (indicated by an asterisk), it is monophyletic when the infraspecific phylogeny of *N. standleyi* is inferred using four plastid markers (Fig. 2).

Currently, we have only three confirmed records for clade C, two from Oaxaca and one from Puebla, Mexico. Samples from this region were assigned to the Y chemotype by Siegler and Wollenweber (1983) on the basis of their light-colored farina. However, our plastid phylogeny suggests with robust support that clade C is sister to the clade formed by chemotypes G and Y (Fig. 2). Our nuclear phylogenies also support that they are a molecularly distinct group within *N. standleyi* (Fig. 4).

Clade G is identical to the G chemotype as recognized by Seigler and Wollenweber (1983). Its distribution is concentrated in the Sonoran Desert and ranges from Arizona and Sonora to Baja California (Fig. 1B). Members of this clade grow almost exclusively on igneous rocks, commonly on granite. Clade Y has the widest distribution range within *N. standleyi* (Fig. 2). Concentrated in the Chihuahuan Desert, it occurs west from eastern Arizona and northeast Sonora, through New Mexico and Chihuahua, and east to Texas and Coahuila. Its northernmost populations are found in Colorado and Oklahoma, and our southernmost confirmed record is in Durango. Like clade G, this chemotype occurs mostly on igneous rocks; it occasionally occurs on limestone as well.

Assessing ploidy

Four individuals included in the phylogenetic analyses provided chromosome counts, and three of them (nos. 1, 7, and 32) showed $n = 30$, the diploid number for *Notholaena*. These three samples represented chemotypes C, G, and Y, and their mean spore diameters were 50.4, 53.1, and 49.3 μm (see Fig. 2 and Table 2), respectively. The fourth plant analyzed chromosomally (no. 18) belonged to chemotype P and showed $n = 60$, indicating that it was a tetraploid; its mean spore diameter was 61.3 μm.

The ploidy levels for the other 35 samples with mature spores were inferred by comparing relative spore sizes with the four samples calibrated by chromosome counts (Fig. 2; Table 2). The means and standard deviations of spore diameters from 25 spores (for each sample) are listed in Table 2; their median, first quartile, and third quartile were plotted as box plots. Samples with mean spore diameters of 48–54 μm were inferred to be diploid, whereas samples with mean spore diameters of 60–63 μm were inferred to be tetraploid. These data indicate that all samples of chemotypes C, G, and Y are diploid and that all P and YG samples are tetraploid (Fig. 2; Table 2). All specimens of *N. standleyi* included in the analyses yielded 32 spores per sporangium, with the exception of one YG sample from Otero County, New Mexico (no. 14). On this specimen, one sampled sporangium produced 32 spores with a mean spore diameter of 60.60 ± 1.76; the remainder contained just 16 spores averaging ~70 μL in diameter (Table 2; Fig. 2). The larger spores from the 16-spored sporangia may be unreduced, resulting from a premeiotic endomitosis.

Biochemical comparisons

Ten different compounds were isolated from sporophytic farina deposits by our TLC analyses. The relative intensity of the compounds was scored by eye into five categories ranging from "absent" to "very strong," and these observations were recorded as " ", "+", "++", "+++", and "++++", respectively (Table 3). Chemotypes G, Y, and YG, the three initially recognized by Seigler and Wollenweber (1983), were weakly clustered on the PCA plot (Fig. 5A) with the 16 reference samples derived from their study (indicated by collector and collection number in Fig. 5). Separation among these three chemotypes was much clearer on the LDA plot (Fig. 5B), which is the focus of the following observations. Four samples considered "anomalous" YG by Seigler and Wollenweber (1983) have a much paler farina than YG and are distributed southwest of the main range of that chemotype. Spore data were available for one of these YG? samples (Correll and Gentry 22759, from LL), which had 32 spores per sporangium, and a spore diameter of 49.57 ± 2.24 μm, very similar to chemotype Y. Although we were unable to isolate DNA from any specimens annotated as such (anomalous YG; samples nos. 30–34 in Seigler and Wollenweber, 1983), we did obtain a *trnG-trnR* sequence from one sample from southern Chihuahua that has a similar farina color (R.A.Bye 10058, DB#13652 [Appendix 1]). In our *trnG-trnR* phylogeny (Fig. 1), this sample is nested within chemotype Y. When flavonoid data for the four YG? samples were mapped on the LDA plot (Fig. 5B), they clustered with Y rather than YG. Among the three plants belonging to the newly recognized cryptic (C) clade, the two samples collected in Oaxaca (nos. 1 and 2) clustered with chemotype group Y, whereas the sample collected from Puebla (no. 3) clustered with YG (Fig. 5). Likewise, most samples of chemotype P clustered with chemotype Y (except for sample no. 19 from Caborca, Sonora, which grouped with YG), reflecting the fact that P usually produces a lighter farina similar to Y.

DISCUSSION

Diversification of *Notholaena standleyi*

In this study, we identify four clades and five chemotypes within *N. standleyi* (Figs. 2 and 4) that differ in geographic range, ploidy, substrate preference, and farina chemistry. Here, we discuss the potential roles of these factors on the infraspecific diversification of *N. standleyi*.

Geographic isolation—The distribution of the three extant diploid clades (C, G, and Y) of *N. standleyi* suggests that geographic isolation has played an important role in their diversification. The divergence between clade C and the clade formed by Y and G (Fig. 3)

TABLE 2. Voucher info, Fern Lab Database (DB) number (http://fernlab.biology.duke.edu/), spore diameter, inferred ploidy level, the alleles/homeologs amplified for each molecular marker and the chemotype group they belong to (see groups in Fig. 4), and the inferred chemotypes. Spore sizes of chromosome vouchers are in bold. Asterisks indicate groups that are not monophyletic.

Series no.	Voucher	Fern DB no.	Spore size (µm)	Ploidy	Plastid	*ApPEFP_C*	*gapCpSh*	*IBR3*	*SQD1*	*transducin*	Chemotype
1	M.D.Windham 525	4548	50.40 ± 0.79	2[a]	C	C	C		C	C*	Cryptic
2	G.Yatskievych 83-139	13646	50.77 ± 1.06	2	C	C	C		C	C*	Cryptic
3	P.Tenorio L. 8810	13657	50.80 ± 0.96	2	C	C	C		C + C	C*	Cryptic
4	E.Schuettpelz 435	3142	53.67 ± 2.07	2	G	G	G	G*	G* + G*		Gold
5	C.J.Rothfels 2546	5438	Immature	–	G	G + G	G	G*	G* + G*		Gold
6	T.-T.Kao 17-002	13417	52.90 ± 1.90	2	G	G + G	G	G* + G*	G*	G	Gold
7	T.-T.Kao 17-004	13419	53.07 ± 2.09	2[b]	G	G	G	G*	G* + G*	G	Gold
8	T.-T.Kao 17-006	13420	53.08 ± 1.52	2	G	G + G		G* + G*	G*	G	Gold
9	T.-T.Kao 17-005	13430	53.31 ± 1.68	2	G	G	G	G*	G* + G*	G + G	Gold
10	B.T.Wilder 07-542	13490	Immature	–	G	G	G	G* + G*	G*	G	Gold
11	S.Carnahan SC 966	13492	51.68 ± 1.17	2	G	G + G	G	G* + G*	G* + G*	G + N	Gold
12	S.Carnahan SC 706	13500	52.26 ± 1.26	2	G	G	G	G*	G*	G	Gold
13	T.L.Burgess 6489	13506	51.91 ± 1.83	2	G	G	G	G* + G*	G* + G*	G + G	Gold
14	C.J.Rothfels 2501	5374	60.60 ± 1.76	4	P/YG	P/YG1 + P/YG2	P/YG + YG	P/YG2	P/YG1 + P/YG2	P/YG1 + YG	Pallid
15	C.J.Rothfels 2535	5419	60.71 ± 0.99	4	P/YG	P/YG1 + P/YG2	P	P/YG1 + P/YG2			Pallid
16	C.J.Rothfels 2537	5422	61.39 ± 1.82	4	P/YG	P/YG1 + P/YG2	P/YG + P	P/YG2	P/YG1 + P/YG2	P/YG1 + P	Pallid
17	T.-T.Kao 17-008	13422	62.67 ± 1.32	4	P/YG	P/YG1 + P/YG2	P/YG + P	P/YG2	P/YG1 + P/YG2	P/YG1 + P	Pallid
18	T.-T.Kao 17-010	13424	61.32 ± 1.11	4[b]	P/YG	P/YG1 + P/YG2	P/YG + P	P/YG2	P/YG1 + P/YG2	P/YG1 + P	Pallid
19	T.L.Burgess 6351	13507	60.37 ± 1.74	4	P/YG	P/YG1 + P/YG2			P/YG1 + P/YG2	P/YG1 + P	Pallid
20	P.C.Fischer 82-11	13645	60.93 ± 1.40	4	P/YG	P/YG1 + P/YG2	P/YG + P	P/YG2	P/YG1 + P/YG2	P/YG1 + P	Pallid
21	J.Metzgar 129	3783	48.46 ± 1.28	2	Y	Y2	Y*	Y2*			Yellow
22	M.D.Windham 94-160	4549	49.04 ± 1.48	2	Y	Y2	Y*	Y1* + Y2*	Y2	Y	Yellow
23	M.D.Windham 94-162	5096	Immature	–	Y	Y2	Y*	Y1* + Y2*	Y2 + Y2	Y	Yellow
24	C.J.Rothfels 2513	5389	Immature	–	Y	Y1 + Y2	Y*	Y2*			Yellow
25	J.Beck 1023	5639	48.29 ± 2.21	2	Y	Y2	Y*	Y2*	Y2	Y	Yellow
26	J.Beck 1025	5641	48.70 ± 1.49	2	Y	Y1 + Y2	Y*	Y1*	Y2	Y	Yellow
27	J.Beck 1046	5662	53.17 ± 2.07	2	Y	Y2	Y*	Y1*	Y2	Y	Yellow
28	T.-T.Kao 17-025	13415	51.86 ± 1.94	2	Y	Y1 + Y2	Y* + N	Y2*	Y2 + Y2	Y	Yellow
29	T.-T.Kao 17-001	13416	49.40 ± 1.60	2	Y	Y2	Y*	Y2*	Y2	Y	Yellow
30	T.-T.Kao 17-013	13425	Sterile	–	Y	Y1 + Y2	Y* + Y*	Y2*	Y2	Y	Yellow
31	T.-T.Kao 17-014	13426	49.68 ± 1.55	2	Y	Y1 + Y2	Y*	Y1* + Y2*	Y2	Y	Yellow
32	T.-T.Kao 17-016	13427	49.30 ± 0.94	2[a]	Y	Y2	Y*	Y1* + Y2*	Y2	Y	Yellow
33	T.-T.Kao 17-017	13428	50.79 ± 1.96	2	Y	Y1 + Y2	Y* + Y*	Y1* + Y2*	Y2	Y	Yellow
34	T.-T.Kao 17-018	13429	49.42 ± 1.38	2	Y	Y1 + Y2	Y*	Y2*	Y2	Y	Yellow
35	T.-T.Kao 17-015	13431	50.50 ± 1.08	2	Y	Y1	Y*	Y1* + Y2*	Y2	Y + Y	Yellow
36	M.K.Terry 908	13435	49.60 ± 1.23	2	Y	Y2	Y* + Y*	Y1* + Y2*	Y2	Y	Yellow
37	M.Schiebout 4838	13463	Released	–	Y	Y2	Y*	Y1* + Y2*	Y2	Y	Yellow
38	T.Reeves 4850	13650	51.91 ± 1.52	2	Y	Y1 + Y1	Y*	Y1* + Y2*	Y2	Y	Yellow
39	T.Reeves 6387	13651	52.47 ± 1.24	2	Y				Y1 + Y2	Y	Yellow
40	B.D.Parfitt 4357	13654	51.20 ± 1.73	2	Y	Y2	Y* + Y*	Y1*	Y1	Y	Yellow
41	M.H.Mayfield et.al. 157	13656	51.58 ± 1.43	2	Y	Y1 + Y2	Y*	Y2*	Y2	Y	Yellow
42	M.D.Windham 94-161	4502	61.38 ± 1.70	4	P/YG	P/YG1 + P/YG2	P/YG + YG	P/YG1 + P/YG2			Yellow-green
43	M.C.Johnston 10467F	13432	62.87 ± 1.46	4	P/YG						Yellow-green
44	J.Fenstermacher 867	13437	Sterile	–	P/YG	P/YG1 + P/YG2	YG	P/YG2	P/YG1 + P/YG2	P/YG1 + YG	Yellow-green
45	J.Henrickson 13716	13448	62.58 ± 1.19	4	P/YG						Yellow-green
46	G.B.Hinton 28435	13457	Immature	–	P/YG	P/YG1 + P/YG2	YG	YG*	P/YG1 + P/YG2	P/YG1 + YG	Yellow-green
47	J.B.Walker 2116	13473	62.05 ± 1.30	4	P/YG	P/YG1 + P/YG2		YG*	P/YG1 + P/YG2	P/YG1 + YG	Yellow-green
48	D.Castillo 1091	13649	61.57 ± 1.65	4	P/YG	P/YG1 + P/YG2	P + YG	YG*	P/YG1 + P/YG2	P/YG1 + YG	Yellow-green

[a]M. D. Windham, unpublished data.
[b]Kao et al., 2019.

may have been driven by long-term allopatry, with clade C confined to Oaxaca and Puebla, separated from the ranges of all other chemotypes by >500 km (Fig. 1). The current distributions of clades G and Y are parapatric, with G concentrated in the Sonoran Desert and Y in the Chihuahuan Desert. There is a small zone of overlap in eastern Arizona (Fig. 1; Appendix 1) where plants of the two chemotypes grow together and hybridize (T.-T. Kao et al., unpublished data). Their estimated divergence time is (1.3)–2.1–(3.1) mya (Fig. 3), which corresponds with hypotheses that the biotic diversification between the two deserts may be attributable to vicariance

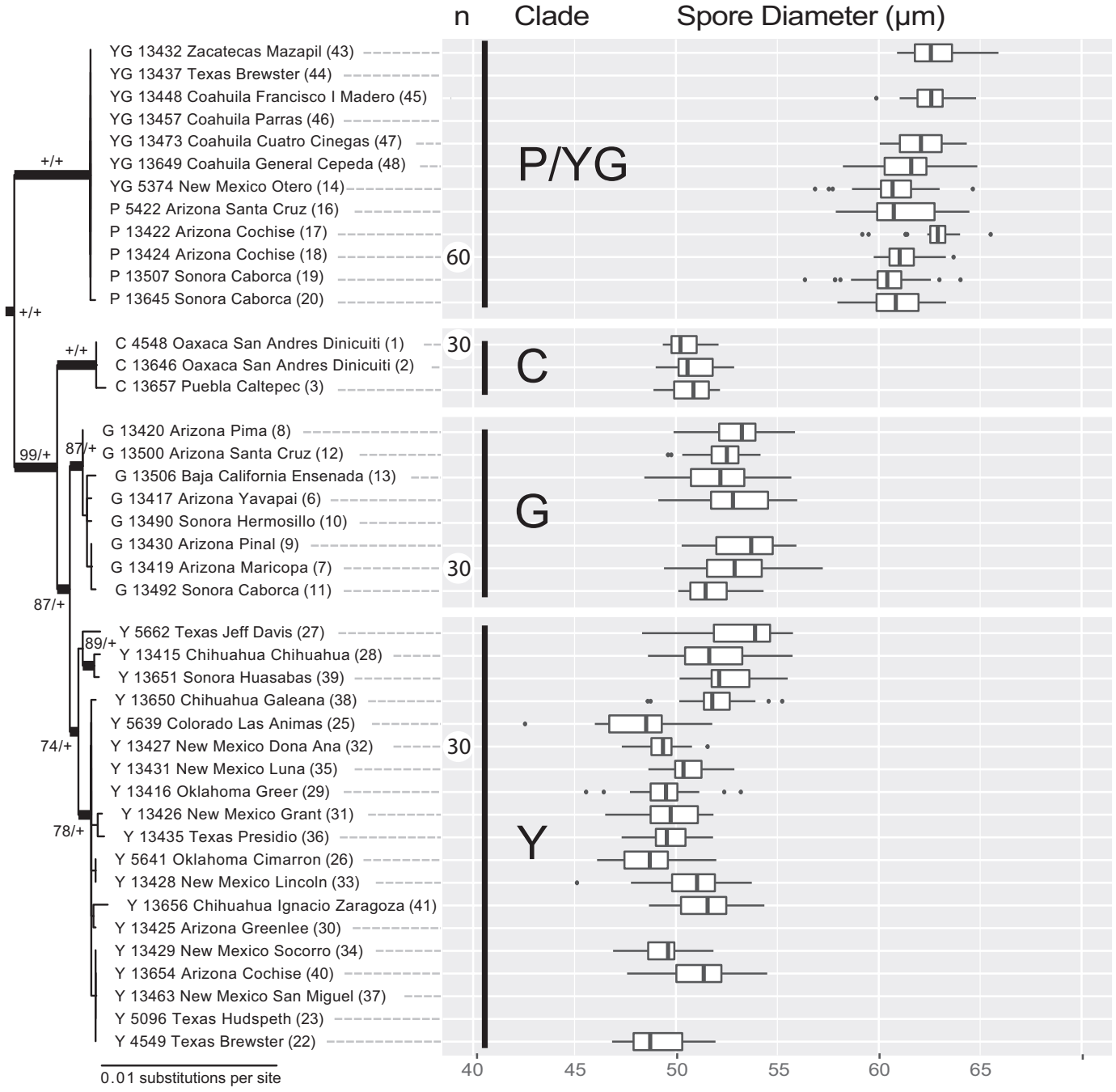

FIGURE 2. Infraspecific phylogeny of *Notholaena standleyi* inferred using four plastid markers (*matK-rps16*, *ndhF*, *trnG-trnR*, and *trnL-trnF*). Four monophyletic groups are recognized: the pallid and yellow-green chemotypes (P/YG); the cryptic clade (C); the gold chemotype (G); and the yellow chemotype (Y). The best maximum likelihood (ML) tree is presented. Branches with ≥70% ML bootstrap support and ≥0.95 posterior probability (PP) are thickened and the support values (ML bootstrap/PP) are shown on the branches. Plus signs indicate that the ML bootstrap = 100% or PP = 1. Chromosome counts (when available) are presented in black circles after sample names. In notholaenids, $n = 30$ is sexual diploid; $n = 60$ is sexual tetraploid. The range of spore diameters for each sample with mature spores is displayed using a box plot at the right side of the plastid phylogeny.

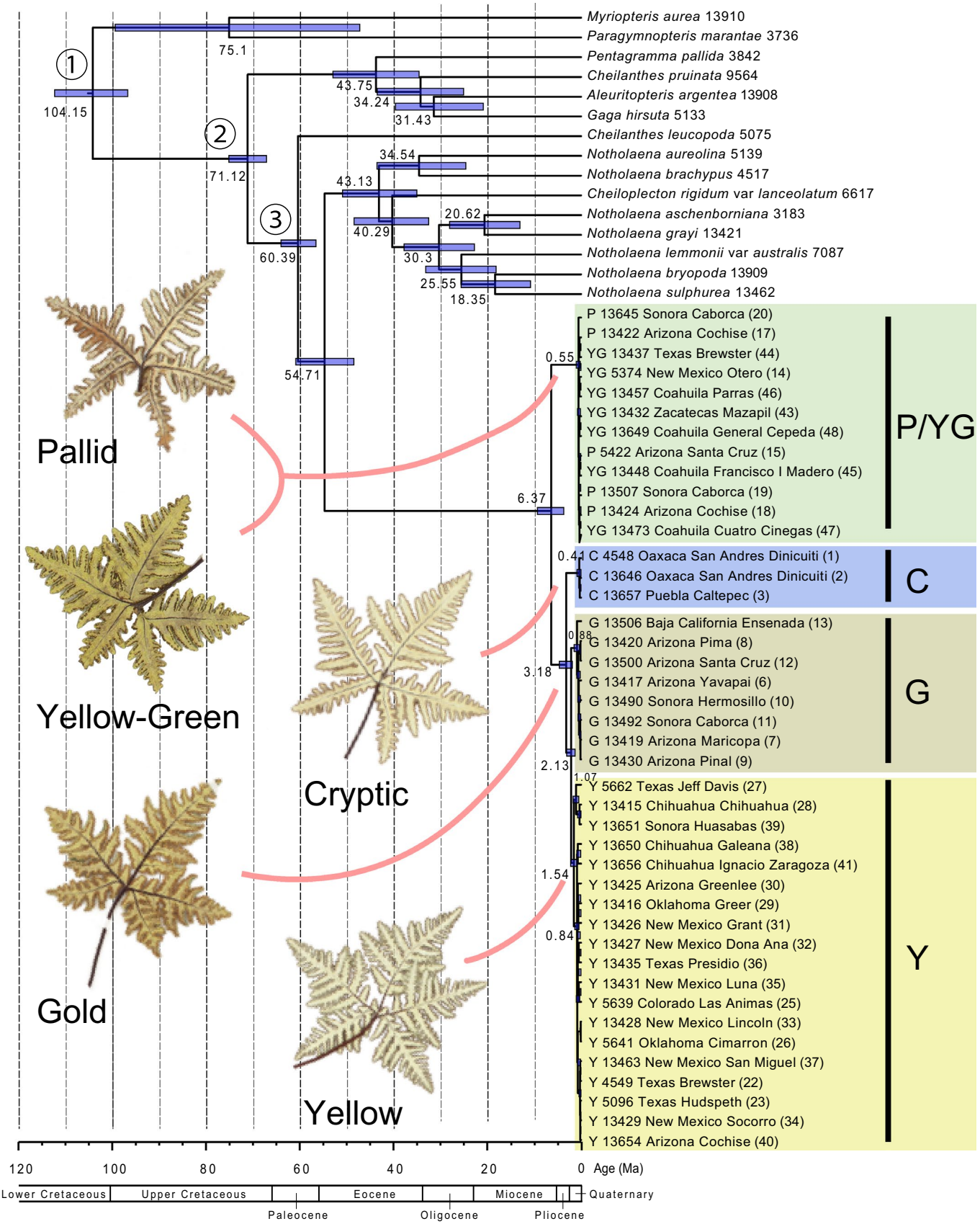
Myriopteris aurea 13910
Paragymnopteris marantae 3736
Pentagramma pallida 3842
Cheilanthes pruinata 9564
Aleuritopteris argentea 13908
Gaga hirsuta 5133
Cheilanthes leucopoda 5075
Notholaena aureolina 5139
Notholaena brachypus 4517
Cheiloplecton rigidum var lanceolatum 6617
Notholaena aschenborniana 3183
Notholaena grayi 13421
Notholaena lemmonii var australis 7087
Notholaena bryopoda 13909
Notholaena sulphurea 13462
1
2
3
104.15
75.1
71.12
60.39
54.71
43.75
34.24
31.43
34.54
43.13
40.29
20.62
30.3
25.55
18.35
0.55
6.37
0.41
0.88
3.18
2.13
1.07
1.54
0.84
P 13645 Sonora Caborca (20)
P 13422 Arizona Cochise (17)
YG 13437 Texas Brewster (44)
YG 5374 New Mexico Otero (14)
YG 13457 Coahuila Parras (46)
YG 13432 Zacatecas Mazapil (43)
YG 13649 Coahuila General Cepeda (48)
P 5422 Arizona Santa Cruz (15)
YG 13448 Coahuila Francisco I Madero (45)
P 13507 Sonora Caborca (19)
P 13424 Arizona Cochise (18)
YG 13473 Coahuila Cuatro Cinegas (47)
P/YG
C 4548 Oaxaca San Andres Dinicuiti (1)
C 13646 Oaxaca San Andres Dinicuiti (2)
C 13657 Puebla Caltepec (3)
C
G 13506 Baja California Ensenada (13)
G 13420 Arizona Pima (8)
G 13500 Arizona Santa Cruz (12)
G 13417 Arizona Yavapai (6)
G 13490 Sonora Hermosillo (10)
G 13492 Sonora Caborca (11)
G 13419 Arizona Maricopa (7)
G 13430 Arizona Pinal (9)
G
Y 5662 Texas Jeff Davis (27)
Y 13415 Chihuahua Chihuahua (28)
Y 13651 Sonora Huasabas (39)
Y 13650 Chihuahua Galeana (38)
Y 13656 Chihuahua Ignacio Zaragoza (41)
Y 13425 Arizona Greenlee (30)
Y 13416 Oklahoma Greer (29)
Y 13426 New Mexico Grant (31)
Y 13427 New Mexico Dona Ana (32)
Y 13435 Texas Presidio (36)
Y 13431 New Mexico Luna (35)
Y 5639 Colorado Las Animas (25)
Y 13428 New Mexico Lincoln (33)
Y 5641 Oklahoma Cimarron (26)
Y 13463 New Mexico San Miguel (37)
Y 4549 Texas Brewster (22)
Y 5096 Texas Hudspeth (23)
Y 13429 New Mexico Socorro (34)
Y 13654 Arizona Cochise (40)
Y
Pallid
Yellow-Green
Cryptic
Gold
Yellow
120
100
80
60
40
20
0
Age (Ma)
Lower Cretaceous
Upper Cretaceous
Eocene
Miocene
Quaternary
Paleocene
Oligocene
Pliocene

FIGURE 3. Chronogram for *Notholaena standleyi* inferred using four plastid markers (*matK-rps16*, *ndhF*, *trnG-trnR*, and *trnL-trnF*). The 95% highest posterior densities of divergence dates are shown as blue bars, and the mean divergence times for critical nodes are indicated. Three nodes that were secondarily calibrated using the divergence times estimated by Testo and Sundue (2016) are denoted by circled numbers 1–3. The chemotypes/clades are summarized at the right side of the chronogram (C = cryptic, G = gold, P = pallid, Y = yellow, YG = yellow-green). Abaxial snapshots of abaxial leaf surfaces for each chemotype are displayed at the lower left of the chronogram (vouchers: C: *Windham 525*; G: *Schuettpelz 435*; P: *Fischer 82-11*; Y: *Windham 96-312*; YG: *Windham 94-161*).

events occurring between the late Neogene and the late Pleistocene (Morafka, 1977; Riddle and Hafner, 2006). These events include the uplifting of the Sierra Madre Occidental in the Neogene and the closure of the Deming Plains during periods of climate cooling in the Pleistocene.

Polyploidy—Whole-genome duplication or polyploidy is a highly effective trigger for species diversification (Otto and Whitton, 2000; Rothfels and Otto, 2016) because it immediately reduces compatibility between parental lineages and their descendants. Polyploids are especially common in ferns, where they comprise at least one-third of extant diversity (Wood et al., 2009). Classification of polyploids is often based on the relationships of their parents; polyploid lineages arising from hybridization between different species are referred to as allopolyploids, whereas those arising within a single species are called autopolyploids (e.g., Spoelhof et al., 2017). Although this distinction is often blurred by contested species concepts, it is useful to know where a given taxon falls on the autopolyploid vs. allopolyploid spectrum. In the case of *N. standleyi*, we hypothesize that the tetraploid chemotypes fall on the autopolyploid side. We base this inference on (1) the scarcity and subtlety of the morphological characters distinguishing the diploid and tetraploid chemotypes, and (2) the phylogenetic isolation of *N. standleyi* from all morphologically similar species (core *Notholaena* in Figs. 1–4).

Narrower definitions of autopolyploidy have been espoused by some authors, such as focusing application of the term on organisms that form multivalents during meiosis (Jackson and Casey, 1980, 1982) or that show evidence of polysomic inheritance (Soltis and Rieseberg, 1986). In the one plant of chemotype P cytogenetically analyzed so far, there was no evidence of multivalent formation; spore mother cells uniformly produced 60 paired chromosomes during meiosis I (Kao et al., 2019). In terms of polysomic inheritance, three of the nuclear markers included in our study (*ApPEFP_C*, *SQD1*, and *transducin*) appear to be strictly disomic; every individual of the tetraploid chemotypes P and YG shows two alleles (labeled "a" and "b" in Fig. 4A, D, E) derived from two different clades. As noted earlier, the departure from this pattern seen in *IBR3* (where most samples show a single allele traceable to chemotype Y; Fig. 4C) is likely due to failed amplification of alleles from the P/YG1 ("a" allele) clade in most individuals. However, the pattern observed in *gapCpSh* could be the result of polysomic inheritance. In this marker, four individuals lack "a" alleles; three of these (P-15, YG-44, YG-46) show a single "b" allele while the fourth (YG-48) exhibits two different "b" alleles. The intriguing possibility of polysomic inheritance in *N. standleyi* should be investigated further by direct sequencing of spores or gametophytes derived from sporophytes with known heterozygous genotypes.

Substrate preference—One major challenge for recently formed polyploids to survive and prosper is their potential to introgress with their parents, which can result in extinction due to minority cytotype exclusion (Levin, 1975). Ranges of the tetraploid chemotypes P and YG are parapatric with those of diploid clades G and Y, respectively (Fig. 1). However, P and YG apparently grow only on limestone, whereas Y and G grow almost exclusively on igneous and non-calcareous sedimentary rocks. Mixed populations involving chemotype P are unknown, and a single hybrid between YG and Y has been documented from west Texas (T.-T. Kao et al., unpublished data). Thus, it appears that substrate preference could play a significant role in the reproductive isolation of chemotypes P and YG from these geographically proximate diploids, thus increasing the probability of survival for newly formed tetraploid lineages. Similar evolutionary patterns have been reported in *Asplenium trichomanes* (Lovis, 1978; Tigerschiold, 1981; Moran, 1982; Liu et al., 2018). In this species, the globally distributed diploid (subsp. *trichomanes*) avoids limestone, while the four recognized tetraploid subspecies are mostly restricted to limestone. A recent molecular study by Liu et al. (2018) found that all tetraploids share plastid haplotypes with the diploid European limestone endemic subsp. *inexpectans*, which suggests that the latter is their maternal parent. The situation in *N. standleyi* is very similar. Here, the calcicolous tetraploid chemotypes (P and YG) are surrounded by an abundance of limestone-avoiding diploids, and their preference for limestone substrates remains unexplained. However, their shared maternal parent has so far eluded detection, and a thorough sampling of spore sizes from populations growing on limestone in the Chihuahuan Desert will almost certainly yield the *N. standleyi* version of subsp. *inexpectans*.

Farina chemistry—The farina chemistry of chemotypes G and Y is quite different (Fig. 5; Table 3). Our results support the conclusion of Seigler and Wollenweber (1983) that there is a definite genetic basis for the separation. Plants of the two chemotypes were grown side-by-side for nearly two years in the Duke University greenhouses, and the farina color and chemistry of newly produced leaves remained unchanged (Appendix S2). It is unclear at this point whether these differences are adaptive or selectively neutral, but it is conceivable they could play a role in reproductive isolation of chemotypes G and Y. Notholaenids are the only ferns well documented to produce farina on both sporophytes and gametophytes (Johnson et al., 2012). On sporophytes, the farina forms a dense layer on abaxial leaf surfaces that may reduce water loss from transpiration and/or protect dry, dormant leaves from UV damage (Hevly, 1963; Wollenweber, 1984). The scattered, farina-producing trichomes along the margins of gametophytes in *N. standleyi* and many other notholaenids would provide neither of these functions. However, gametophytic farina could play a role in sexual reproduction, potentially providing a chemical attractant to spermatozoids of genetically compatible individuals and/or a repellant to those of other taxa. This might help explain the divergence of chemotypes G and Y in *N. standleyi* as well as the relative rarity of interspecific hybridization in *Notholaena* (Kao et al., 2019) compared to the myriopterid (Grusz et al., 2014) and pellaeid (Windham, 1993b) lineages of cheilanthoid ferns.

CONCLUSIONS

Our molecular, cytological, biochemical, and biogeographical analyses of *N. standleyi* reveal some intriguing patterns. The species is strongly supported as monophyletic, though its phylogenetic position in relation to other notholaenid ferns remains unresolved. Our sampling encompasses five recognizable genetic groupings that began diverging ~6.4 mya (95% HPD 3.7–9.3 mya). These include three diploid clades (C, G, and Y) as well as two tetraploid chemotypes (P and YG) that likely arose through separate hybridization events. A surprising variety of mechanisms have played a role in the divergence of these taxa. Clade C is geographically isolated from all other members of the species, and we hypothesize that the split between this and the sister G + Y clade at ~3.2 mya (95% HPD 1.9–4.6 mya) was driven by allopatry. Chemotypes G and Y are largely confined to the Sonoran and Chihuahuan deserts, respectively, but they do co-occur and hybridize (T.-T. Kao et al., unpublished data) in the narrow ecotone between these deserts. We suspect that these clades have undergone parapatric differentiation as the two deserts diverged over the course of the Pleistocene (2.1 mya (95% HPD [1.3–3.1 mya]). Finally, chemotypes P and YG represent tetraploid hybrids between a missing diploid maternal parent sister to all other extant populations and paternal parents nested within or closely related to chemotype Y. In the nuclear marker *transducin* (Fig. 4E), the paternal alleles of P and YG form distinct groups, reinforcing the original separation based on farina color and suggesting that these two chemotypes originated from different hybridization events. Chemotypes P and YG are only known to occur on

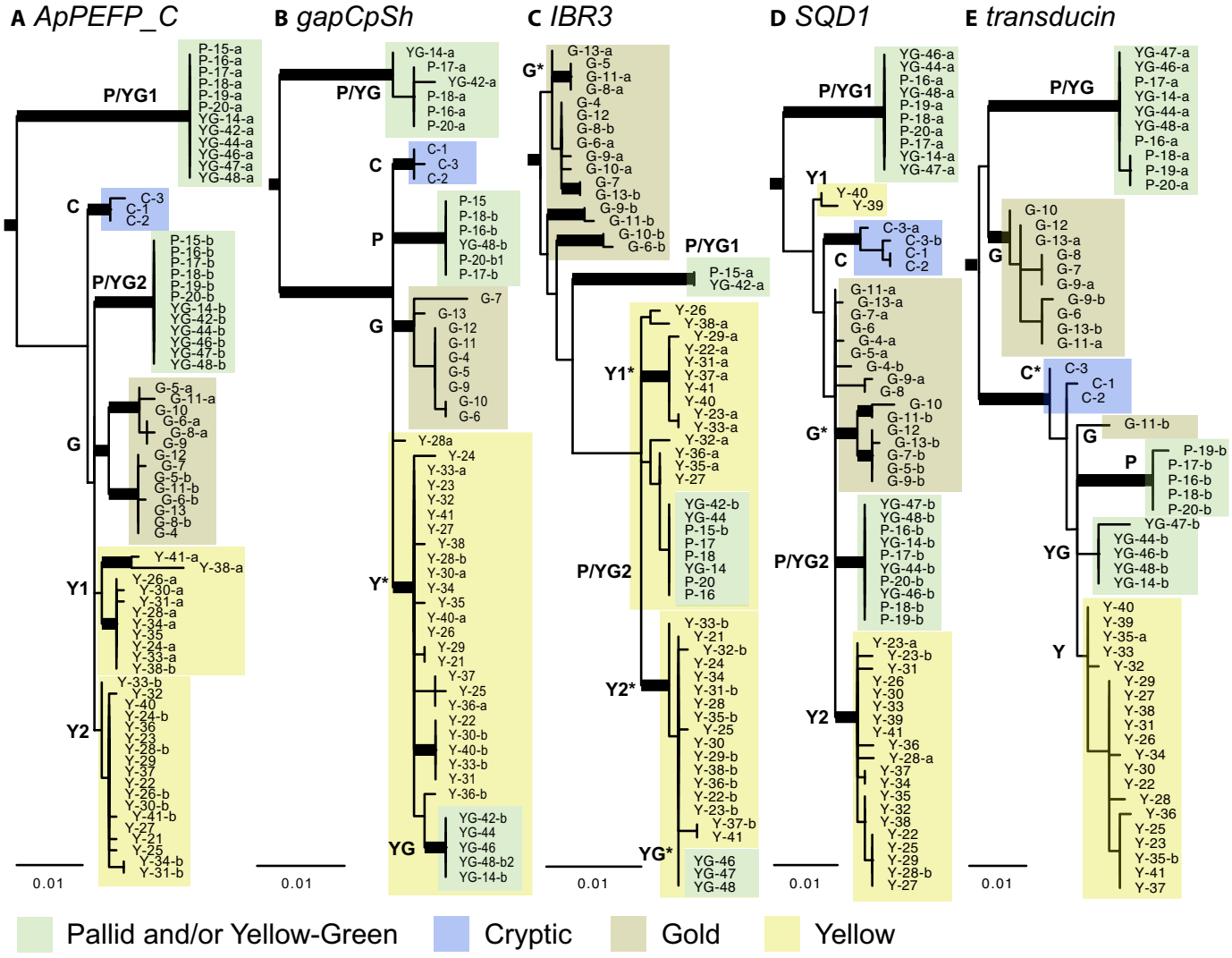

FIGURE 4. Nuclear phylogenies for *Notholaena standleyi* inferred from five different molecular markers. (A) *ApPEFP_C*; (B) *gapCpSh*; (C) *IBR3*; (D) *SQD1*; (E) *transducin*. The best maximum likelihood (ML) tree for each marker is presented. Branches with ≥70% ML bootstrap support and ≥0.95 posterior probability (PP) are thickened. Sample names are indicated using the format "chemotype-series #". Chemotypes: C = cryptic, G = gold, P = pallid, Y = yellow, YG = yellow-green. When a sample has two copies, these are identified as "a" or "b" after the sample name. Vouchers associated with the series numbers are listed in Table 2. Recognized chemotypes within the trees are highlighted by colored blocks (see legend at bottom of figure), and an abbreviated name is assigned to each group (near the base of each group). Non-monophyletic groups are indicated with an asterisk. Scale bars indicate 0.01 substitutions per site.

TABLE 3. Chemical composition of farina of selected *Notholaena standleyi* specimens. The sample numbers are either the series number from Table 2 or the sample number in Seigler and Wollenweber (1983: table 1; indicated as S-#).

			Compound									
Sample no.	**Voucher**	**Chemotype**	**1**	**2**	**3**	**4**	**5**	**6**	**7**	**8**	**9**	**10**
1	M.D.Windham 525	Cryptic				++	++	++		+++++	+++	
2	G.Yatskievych 83-139	Cryptic					+			+++++	+++	
3	P.Tenorio L. 8810	Cryptic	++		+++	+++	++		++	+++		++
6	T.-T.Kao 17-002	Gold		+	++++	+++	++++	++	++++			
7	T.-T.Kao 17-004	Gold			+++	+++	+++	++	+++			
8	T.-T.Kao 17-006	Gold			+++	+++	+++	++	+++			
9	T.-T.Kao 17-005	Gold			+++	+++	++++	++	+++			
10	B.T.Wilder 07-542	Gold			++	+++	++++	++	+++			
11	S.Carnahan SC 966	Gold			++	+++	++++	++	+++			
12	S.Carnahan SC 706	Gold			++	+++	++++	++	++			
13	T.L.Burgess 6489	Gold			++	++	++++		+++			
14	C.J.Rothfels 2501	Yellow-green								+++++	++	
16	C.J.Rothfels 2537	Pallid					+			+++++	+++	
17	T.-T.Kao 17-008	Pallid	++		++++	++++				++++		
18	T.-T.Kao 17-010	Pallid								+++++		
19	T.L.Burgess 6351	Pallid			++	+++	+++		++	++	+	
20	P.C.Fischer 82-11	Pallid			++	++++	+++			++		+
22	M.D.Windham 94-160	Yellow								+++++		
23	M.D.Windham 94-162	Yellow								+++++		
25	J.Beck 1023	Yellow	+		+++	++++				++++		
26	J.Beck 1025	Yellow			+	++				++++		
27	J.Beck 1046	Yellow				+				+++++		
28	T.-T.Kao 17-025	Yellow			+					+++++	+	
29	T.-T.Kao 17-001	Yellow								++++		
30	T.-T.Kao 17-013	Yellow			+	+++	++			+++++		
31	T.-T.Kao 17-014	Yellow			++	+++	++			+++++	++	
32	T.-T.Kao 17-016	Yellow								+++++	+	
33	T.-T.Kao 17-017	Yellow				++				+++++		
34	T.-T.Kao 17-018	Yellow				++				+++++		
35	T.-T.Kao 17-015	Yellow			+	+++	++			+++++	++	
36	M.K.Terry 908	Yellow			+	+++	++			+++++	++	
37	M.Schiebout 4838	Yellow			++	+++				++++	++	
38	T.Reeves 4850	Yellow								++++	+	
39	T.Reeves 6387	Yellow	++++	++	+++	++	++++	++				
40	B.D.Parfitt 4357	Yellow	++++	+	+++	++	+++					
41	M.H.Mayfield et.al. 157	Yellow	+++	++	++	+++				++++		
43	M.C.Johnston 10467F	Yellow-green	++	+	+++	+++	++++		++	+++		++
44	J.Fenstermacher 867	Yellow-green	++		+++	+++	+++		++	+++		++
45	J.Henrickson 13716	Yellow-green					++		+	+++		
46	G.B.Hinton 28435	Yellow-green			+	++	+++		+	+++		
47	J.B.Walker 2116	Yellow-green			++	++	++		++	++		
48	D.Castillo 1091	Yellow-green	++		+++	+++	+++		+++	+++		++
S-04	Stewart 624	Yellow								+++++		
S-10	Waterfall 7242	Yellow			+	++	++			++++	+	
S-12	Oliver 544	Yellow								+++++	+	
S-16	Correll 30599	Yellow			++	+++				++++	+	
S-29	Correll 22690	Yellow-green			+	+	++		++	+++		
S-30	Knobloch 782	Yellow-green?			+	++++	+++			++		
S-31	Knobloch 8300	Yellow-green?			+	++++	++++			+		
S-32	Knobloch 1854	Yellow-green?			+++	++++	++++			++		
S-33	Correll 22759	Yellow-green?			++	++++			++	+++		+
S-35	Stanford 89	Yellow-green			+	++	++		+++	++		
S-37	Correll 12896	Yellow-green					++		++	+++		
S-40	Keil 6003	Yellow-green	++		++	++	+++		+++	+++		++
S-44	Shreve 7042	Gold			+++	+++	+++	++	+++			
S-46	Keil 2826	Gold			+++	++	++++	++	++	+		
S-50	Walter 2281	Gold		+	+++	+++	++++	++	+++	+		
S-55	Simmons s.n.	Gold			+++	++++	++++	+++	+++			++

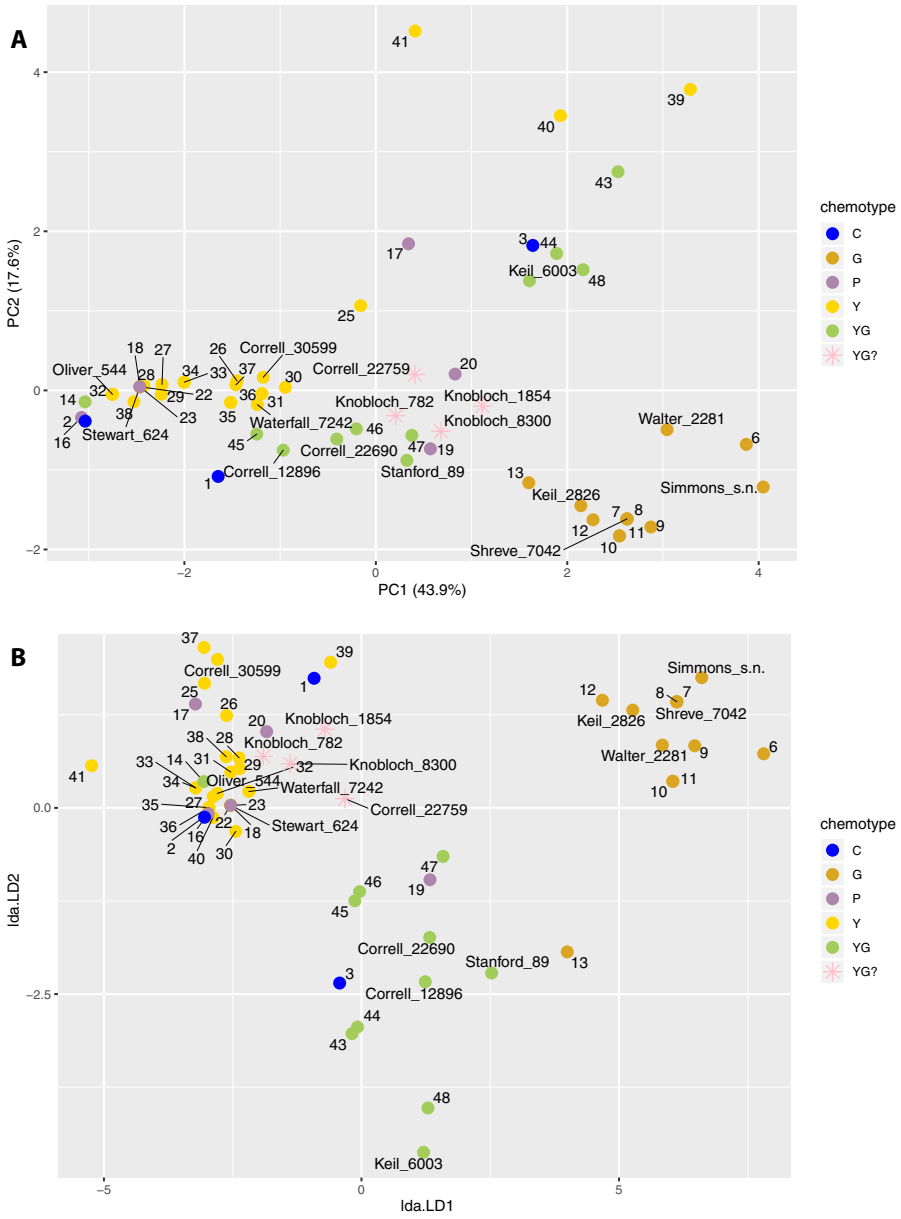

FIGURE 5. Comparison of thin layer chromatography (TLC) results for *Notholaena standleyi*. (A) Principal component analysis and (B) linear discriminant analysis plots of the TLC data. Chemotypes are coded with colors and symbols (see legends to the right of the plots). Chemotypes: C = cryptic, G = gold, P = pallid, Y = yellow, YG = yellow-green, YG? = anomalous yellow-green (*sensu* Seigler and Wollenweber, 1983). The 16 reference samples from Seigler and Wollenweber (1983) are identified by collector and collection number. All other samples are indicated by their series numbers in this study (Table 2).

limestone, and this substrate endemism was likely inherited from the missing maternal parent because the three known diploids generally avoid this substrate. However, chemotype Y is occasionally found on limestone, which could facilitate the co-occurrence of the missing maternal parent of P and YG with the Y-related paternal lineages. The origins of the tetraploid chemotypes P and YG are thus sympatric, and genetic interchange with the diploid clades is apparently limited by a combination of ploidy and substrate preference.

ACKNOWLEDGMENTS

The authors thank G. Alexander, N. Devos, and other staff at the Duke Center for Genomic and Computational Biology for preparing the PacBio library from amplicons and ensuring the success of our PacBio sequencing run. We are grateful to S. LaGreca and D. Armaleo for instruction on the TLC analyses and for loaning equipment; P. Alexander, D. Bailey, M. Barnes, J. Beck, A. Eily, S. Fuentes-Soriano, G. Gile, N. Hernández, L. Huiet, J. Metzgar, M. Moore, M. Powell, E. Schuettpelz, and G. Yatskievych for generously providing material and/or assistance in research and sample collections; the herbaria ARIZ, ASU, CAS, DUKE, IND, MEXU, MICH, MO, OKL, SRSC, TEX/LL, UNM, UC, and US for specimen loans; and the Southwestern Region Office of the U.S. Department of Agriculture, the Arizona State Office of the Bureau of Land Management, and Investigación y Manejo para la Conservación for approving collecting permits and/or assistance in sample collections. This study would not have been possible without the generosity of these individuals, herbaria, and institutes. We also thank the reviewers for their helpful comments and efforts toward improving our manuscript. This research was partly funded by the U.S. National Science Foundation (award DEB-1701942 to K.P. and T.-T.K.) and the American Society of Plant Taxonomists. T.-T.K. thanks the Taiwan Ministry of Education and Duke University for financial support.

AUTHOR CONTRIBUTIONS

M.D.W., C.J.R., and T.-T.K. conceived the idea. M.D.W., C.J.R., and A.M.-C. helped with sample collection. C.J.R. extracted DNA from some of the samples and provided support for the molecular analyses. M.D.W. did the chromosome analyses. T.-T.K. carried out the experiments and analyzed and curated the data. T.-T.K. and M.D.W. wrote the manuscript. K.M.P. supervised the project. All authors discussed the results and contributed to the final manuscript.

DATA AVAILABILITY

All data sets and phylogenetic trees are deposited in the TreeBASE: http://purl.org/phylo/treebase/phylows/study/TB2:S25579.

SUPPORTING INFORMATION

Additional Supporting Information may be found online in the supporting information tab for this article.

APPENDIX S1. Partitions and evolutionary models used in phylogenetic analyses.

APPENDIX S2. Thin-layer chromatograph (TLC) comparison of the farinose flavonoids of the two diploid chemotypes, "G" and "Y".

LITERATURE CITED

Beck, J. B., M. D. Windham, G. Yatskievych, and K. M. Pryer. 2010. A diploids-first approach to species delimitation and interpreting polyploid evolution in the fern genus *Astrolepis* (Pteridaceae). *Systematic Botany* 35: 223–234.

Benham, D. M. 1988. Chromosome number reports XCIX Á. Löve [ed.],. *Taxon* 37: 396–399.

Bouckaert, R., J. Heled, D. Kühnert, T. G. Vaughan, C.-H. Wu, D. Xie, M. A. Suchard, et al. 2013. Beast2: a software platform for Bayesian evolutionary analysis. *PLoS Computational Biology* 10: 1003537.

DNASTAR. 2019. SeqMan Pro. Version 16.0.0.

Edgar, R. C. 2004. MUSCLE: Multiple sequence alignment with high accuracy and high throughput. *Nucleic Acids Research* 32: 1792–1797.

Edgar, R. C. 2010. Search and clustering orders of magnitude faster than BLAST. *Bioinformatics* 26: 2460–2461.

Grusz, A. L., M. D. Windham, and K. M. Pryer. 2009. Deciphering the origins of apomictic polyploids in the *Cheilanthes yavapensis* complex (Pteridaceae). *American Journal of Botany* 96: 1636–1645.

Grusz, A. L., M. D. Windham, G. Yatskievych, R. L. Huiet, G. J. Gastony, and K. M. Pryer. 2014. Patterns of diversification in the xeric-adapted fern genus *Myriopteris* (Pteridaceae). *Systematic Botany* 39: 698–714.

Hevly, R. H. 1963. Adaptations of cheilanthoid ferns to desert environments. *Journal of the Arizona Academy of Science* 2: 164–175.

Hietz, P. 2010. Fern adaptations to xeric environments. *In* K. Mehltreter, L. R. Walker, and J. M. Sharpe [eds.], Fern Ecology, 140–176. Cambridge University Press, Cambridge.

Jackson, R.C., and J. Casey. 1980. Cytogenetics of polyploids. *In* W. Lewis [ed.], Polyploidy: biological relevance, 17–44, Plenum Publishing Corporation, New York.

Jackson, R. C., and J. Casey. 1982. Cytogenetic analyses of autopolyploids: models and methods for triploids to octoploids. *American Journal of Botany* 69: 489–503.

Johnson, A. K., C. J. Rothfels, M. D. Windham, and K. M. Pryer. 2012. Unique expression of a sporophytic character on the gametophytes of notholaenid ferns (Pteridaceae). *American Journal of Botany* 99: 1118–1124.

Kao, T.-T., K. M. Pryer, F. D. Freund, M. D. Windham, and C. J. Rothfels. 2019. Low-copy nuclear sequence data confirm complex patterns of farina evolution in notholaenid ferns (Pteridaceae). *Molecular Phylogenetics and Evolution* 138: 139–155.

Knobloch, I. W., W. Tai, and T. A. Ninan. 1973. The cytology of some species of the genus *Notholaena*. *American Journal of Botany* 60: 92.

Larsson, A. 2014. AliView: a fast and lightweight alignment viewer and editor for large datasets. *Bioinformatics* 30: 3276–3278.

Levin, D. A. 1975. Minority Cytotype Exclusion in Local Plant Populations. *Taxon* 24: 35–43.

Li, F. W., L. Y. Kuo, Y. M. Huang, W. L. Chiou, and C. N. Wang. 2010. Tissue-direct PCR, a rapid and extraction-free method for barcoding of ferns. *Molecular Ecology Resources* 10: 92–95.

Liu, H. M., S. R. Russell, J. Vogel, and H. Schneider. 2018. Inferring the potential of plastid DNA-based identification of derived ferns: a case study on the *Asplenium trichomanes* aggregate in Europe. *Plant Systematics and Evolution* 304: 1009–1022.

Lovis, J. D. 1978. Evolutionary Patterns and Processes in Ferns. *Advances in Botanical Research* 4: 229–415.

Mickel, J. T., and A. R. Smith. 2004. The Pteridophytes of Mexico. The New York Botanical Garden, New York, Bronx.

Morafka, D. J. 1977. A Biogeographical Analysis of the Chihuahuan Desert through its Herpetofauna. Springer, Netherlands, Dordrecht.

Moran, R. C. 1982. The *Asplenium trichomanes* Complex in the United States and Adjacent Canada. *American Fern Journal* 72: 5.

Nagalingum, N. S., H. Schneider, and K. M. Pryer. 2007. Molecular phylogenetic relationships and morphological evolution in the heterosporous fern genus *Marsilea*. *Systematic Botany* 32: 16–25.

Otto, S. P., and J. Whitton. 2000. Polyploid Incidence and Evolution. *Annual Review of Genetics* 34: 401–437.

PPG I. 2016. A community-derived classification for extant lycophytes and ferns. *Journal of Systematics and Evolution* 54: 563–603.

Proctor, M. C. F., and V. C. Pence. 2002. Vegetative tissues: bryophytes, vascular resurrection plants and vegetative propagules. *In* M. Black and H. W. Pritchard [eds.], Desiccation and survival in plants: Drying without dying, 207–237. CABI Publishing, Wallingford, UK.

Proctor, M. C. F., and Z. Tuba. 2002. Poikilohydry and homoihydry: Antithesis or spectrum of possibilities? *New Phytologist* 156: 327–349.

Rambaut, A., A. J. Drummond, D. Xie, G. Baele, and M. A. Suchard. 2018. Posterior summarization in Bayesian phylogenetics using Tracer 1.7 E. Susko [ed.]. *Systematic Biology* 67: 1–3.

R Development Core Team. 2008. R: A Language and Environment for Statistical Computing. R Foundation for Statistical Computing, Vienna, Austria.

Rhoads, A., and K. F. Au. 2015. PacBio sequencing and its applications. *Genomics, Proteomics and Bioinformatics* 13: 278–289.

Riddle, B. R., and D. J. Hafner. 2006. A step-wise approach to integrating phylogeographic and phylogenetic biogeographic perspectives on the history of a core North American warm deserts biota. *Journal of Arid Environments* 66: 435–461.

Ronquist, F., M. Teslenko, P. van der Mark, D. L. Ayres, A. Darling, S. Höhna, B. Larget, et al. 2012. MrBayes 3.2: efficient Bayesian phylogenetic inference and model choice across a large model space. *Systematic Biology* 61: 539–542.

Rothfels, C. J., and S. P. Otto. 2016. Polyploid speciation. Encyclopedia of Evolutionary Biology, 317–326. Elsevier.

Rothfels, C. J., M. D. Windham, A. L. Grusz, G. J. Gastony, and K. M. Pryer. 2008. Toward a monophyletic *Notholaena* (Pteridaceae): Resolving patterns of evolutionary convergence in xeric-adapted ferns. *Taxon* 57: 712–724.

Rothfels, C. J., A. Larsson, F.-W. Li, E. M. Sigel, L. Huiet, D. O. Burge, M. Ruhsam, et al. 2013. Transcriptome-mining for single-copy nuclear markers in ferns. *PLoS One* 8: e76957.

Rothfels, C. J., K. M. Pryer, and F. W. Li. 2017. Next-generation polyploid phylogenetics: rapid resolution of hybrid polyploid complexes using PacBio single-molecule sequencing. *New Phytologist* 213: 413–429.

Schuettpelz, E., and K. M. Pryer. 2007. Fern phylogeny inferred from 400 leptosporangiate species and three plastid genes. *Taxon* 56: 1037–1050.

Schuettpelz, E., K. M. Pryer, and M. D. Windham. 2015. A unified approach to taxonomic delimitation in the fern genus *Pentagramma* (Pteridaceae). *Systematic Botany* 40: 629–644.

Seigler, D. S., and E. Wollenweber. 1983. Chemical variation in *Notholaena standleyi*. *American Journal of Botany* 70: 790–798.

Sigel, E. M., M. D. Windham, L. Huiet, G. Yatskievych, and K. M. Pryer. 2011. Species relationships and farina evolution in the cheilanthoid fern genus *Argyrochosma* (Pteridaceae). *Systematic Botany* 36: 554–564.

Smith, A. R. 1974. Taxonomic and cytological notes on ferns from California and Arizona. *Madroño* 22: 376–378.

Soltis, D. E., and L. H. Rieseberg. 1986. Autopolyploidy in *Tolmiea menziesii* (Saxifragaceae): evidence from enzyme electrophoresis. *American Journal of Botany* 73: 310–318.

Spoelhof, J. P., P. S. Soltis, and D. E. Soltis. 2017. Pure polyploidy: Closing the gaps in autopolyploid research. *Journal of Systematics and Evolution* 55: 340–352.

Swofford, D. L. 2003. PAUP*. phylogenetic analysis using Parsimony (*and other methods) Version 4. Sinauer, Sunderland, Massachusetts, USA. *Nat. Biotechnol.* 18: 233–234.

Testo, W., and M. Sundue. 2016. A 4000-species dataset provides new insight into the evolution of ferns. *Molecular Phylogenetics and Evolution* 105: 200–211.

Tigerschiold, E. 1981. The *Asplenium trichomanes* complex in East Central Sweden. *Nordic Journal of Botany* 1: 12–16.

Travers, K. J., C. S. Chin, D. R. Rank, J. S. Eid, and S. W. Turner. 2010. A flexible and efficient template format for circular consensus sequencing and SNP detection. *Nucleic Acids Research* 38: e159–e159.

Tryon, A. F. 1947. Glandular prothallia of *Notholaena standleyi*. *American Fern Journal* 37: 88–89.

Wei, R., Y. H. Yan, A. J. Harris, J. S. Kang, H. Shen, Q. P. Xiang, and X. C. Zhang. 2017. Plastid phylogenomics resolve deep relationships among eupolypod II ferns with rapid radiation and rate heterogeneity. *Genome Biology and Evolution* 9: 1646–1657.

Windham, M. D. 1993a. *Notholaena*. *In* Flora of North America editorial committee [ed.],Flora of North America North of Mexico, 143–149. Oxford University Press, New York.

Windham, M. D. 1993b. *Pellaea*. *In* Flora of North America editorial committee [ed.], Flora of North America North of Mexico, 175–186. Oxford University Press, New York.

Windham, M. D., and C. G. Schaack. 1983. Miscellaneous chromosome counts for Adiantaceae, Aspleniaceae, Asteraceae, and Poaceae. *In* Á. Löve [ed.], IOPB chromosome number reports LXXXI. Taxon, 664–665.

Windham, M. D., and G. Yatskievych. 2003. Chromosome studies of cheilanthoid ferns (Pteridaceae: Cheilanthoideae) from the western United States and Mexico. *American Journal of Botany* 90: 1788–1800.

Wollenweber, E. 1984. Exudate flavonoids of Mexican ferns as chemotaxonomic markers. *Rev. Latinoamer. Quim* 15: 11.

Wollenweber, E., and H. Schneider. 2000. Lipophilic exudates of Pteridaceae–chemistry and chemotaxonomy. *Biochemical Systematics and Ecology* 28: 751–777.

Wood, T. E., N. Takebayashi, M. S. Barker, I. Mayrose, P. B. Greenspoon, and L. H. Rieseberg. 2009. The frequency of polyploid speciation in vascular plants. *Proceedings of the National Academy of Sciences* 106: 13875–13879.

Zwickl, D. J. 2006. Genetic algorithm approaches for the phylogenetic analysis of large biological sequence datasets under the maximum likelihood criterion, The University of Texas at Austin.

APPENDIX 1. Information for molecular vouchers and GenBank accession numbers, in the following order: *Species name* [Chemotype], voucher information: country, primary subdivision, secondary subdivision, *Collector & collection number*, herbarium code in Index Herbariorum (http://sweetgum.nybg.org/science/ih/), Fern Lab Database (DB) number (http://fernlab.biology.duke.edu/), and GenBank accession numbers for *trnGR*, *matK-rps16*, *ndhF*, *trnLF*, *ApPEFP_C*, *gapCpSh*, *IBR3*, *SQD1*, and *transducin* (in that order). Individual samples are separated by semicolons. NA = not applicable.

Notholaena standleyi Maxon [Cryptic]: Mexico, Oaxaca, San Andres Dinicuiti, *M.D.Windham 525*, DUKE, DB#4548, MN876592, MN875967, MN876466, MN876675, MN876249, MN876333, NA, MN876732, MN876523; Mexico, Oaxaca, San Andres Dinicuiti, *G.Yatskievych 83-139*, ARIZ, DB#13646, MN876656, MN876002, MN876501, MN876710, MN876300, MN876372, NA, MN876780, MN876569; Mexico, Puebla, Caltepec, *P.Tenorio 8810*, TEX/LL, DB#13657, MN876665, MN876008, MN876507, MN876716, MN876308, MN876379, NA, MN876788 MN876789, MN876576; ***Notholaena standleyi*** Maxon [Gold]: Mexico, Baja California, Ensenada, *T.L.Burgess 6489*, ARIZ, DB#13506, MN876651, MN875999, MN876498, MN876707, MN876295, MN876369, MN876439 MN876440, MN876774 MN876775, MN876563 MN876564; Mexico, Sonora, Caborca, *A.L.Reina-G. 2010-40*, ARIZ, DB#13489, MN876642, NA, NA, NA, NA, NA, NA, NA, NA; Mexico, Sonora, Caborca, *S.Carnahan SC 966*, ARIZ, DB#13492, MN876645, MN875997, MN876496, MN876705, MN876292 MN876293, MN876367, MN876436 MN876437, MN876771 MN876772, MN876560 MN876561; Mexico, Sonora, Guaymas, *Eggli 1966*, MEXU, DB#13474, MN876639, NA, NA, NA, NA, NA, NA, NA, NA; Mexico, Sonora, Guaymas, *R.S.Felger 85-359-A*, ARIZ, DB#13491, MN876644, NA, NA, NA, NA, NA, NA, NA, NA; Mexico, Sonora, Guaymas, *R.S.Felger 95-273*, ARIZ, DB#13505, MN876650, NA, NA, NA, NA, NA, NA, NA, NA; Mexico, Sonora, Hermosillo, *B.T.Wilder 07-542*, ARIZ, DB#13490, MN876643, MN875996, MN876495, MN876704, MN876291, MN876366, MN876434 MN876435, MN876770, MN876559; Mexico, Sonora, Plutarco Elias Calles, *R.S.Felger 89-17*, MEXU, DB#13468, MN876637, NA, NA, NA, NA, NA, NA, NA, NA; Mexico, Sonora, Plutarco Elias Calles, *R.S.Felger 91-11*, ARIZ, DB#13488, MN876641, NA, NA, NA, NA, NA, NA, NA, NA; U.S.A., Arizona, Gila, *J.Metzgar 148*, DUKE, DB#3801, MN876591, NA, NA, NA, NA, NA, NA, NA, NA; U.S.A., Arizona, Gila, *M.D.Windham 94-175*, DUKE, DB#5092, MN876595, NA, NA, NA, NA, NA, NA, NA, NA; U.S.A., Arizona, Graham, *T.-T. Kao 17-011-4*, DUKE, DB#13493, MN876646, NA, NA, NA, NA, NA, NA, NA, NA; U.S.A., Arizona, Maricopa, *T.-T.Kao 17-004*, DUKE, DB#13419, MN876606, MN875978, MN876477, MN876686, MN876265, MN876347, MN876410, MN876747 MN876748, MN876536; U.S.A., Arizona, Maricopa, *M.A.Baker 13711*, ASU, DB#13486, MN876640, NA, NA, NA, NA, NA, NA, NA, NA; U.S.A., Arizona, Maricopa, *R.S.Felger Feb-88*, ARIZ, DB#13503, MN876649, NA, NA, NA, NA, NA, NA, NA, NA; U.S.A., Arizona, Pima, *C.J.Rothfels 2546*, DUKE, DB#5438, MK632841, NA, NA, NA, MK632472 MK632473, MK632598, MK632685, MK632804 MK632805, NA; U.S.A., Arizona, Pima, *T.-T.Kao 17-006*, DUKE, DB#13420, MN876607, MN875979, MN876478, MN876687, MN876266 MN876267, NA, MN876411 MN876412, MN876749, MN876537; U.S.A., Arizona, Pima, *J.Fonseca 2014-350*, ARIZ, DB#13501, MN876648, NA, NA, NA, NA, NA, NA, NA, NA; U.S.A., Arizona, Pinal, *M.D.Windham 94-138*, DUKE, DB#5091, MN876594, NA, NA, NA, NA, NA, NA, NA, NA; U.S.A., Arizona, Pinal, *T.-T.Kao 17-005*, DUKE, DB#13430, MN876615, MN875987, MN876486, MN876695, MN876281, MN876359, MN876423 MN876424, MN876759 MN876760, MN876547 MN876548; U.S.A., Arizona, Santa Cruz, *S.Carnahan SC 706*, ARIZ, DB#13500, MN876647, MN875998, MN876497, MN876706, MN876294, MN876368, MN876438, MN876773, MN876562; U.S.A., Arizona, Yavapai, *E.Schuettpelz 435*, DUKE, DB#3142, EU268705, NA, NA, NA, MK632471, MK632597, MK632684, MK632802 MK632803, NA; U.S.A., Arizona, Yavapai, *T.-T.Kao 17-002*, DUKE, DB#13417, MN876605, MN875977, MN876476, MN876685, MN876263 MN876264, MN876346, MN876408 MN876409, MN876746, MN876535; ***Notholaena standleyi*** Maxon [Pallid]: Mexico, Sonora, Caborca, *T.L.Burgess 6351*, ARIZ, DB#13507, MN876652, MN876000, MN876499, MN876708, MN876296 MN876297, NA, NA, MN876776 MN876777, MN876565 MN876566; Mexico, Sonora, Caborca, *P.C.Fischer 82-11*, ARIZ, DB#13645, MN876655, MN876001, MN876500, MN876709, MN876298 MN876299, MN876370 MN876371, MN876441, MN876778 MN876779, MN876567 MN876568; U.S.A., Arizona, Cochise, *M.D.Windham 94-164*, DUKE, DB#4503, EU268707, NA, NA, NA, NA, NA, NA, NA, NA; U.S.A., Arizona, Cochise, *C.J.Rothfels 2535*, DUKE, DB#5419, MK632842, NA, NA, NA, MK632474 MK632475, MK632599, MK632686 MK632687, NA, NA; U.S.A., Arizona, Cochise, *T.-T.Kao 17-008*, DUKE, DB#13422, MN876608, MN875980, MN876479, MN876688, MN876268 MN876269, MN876348 MN876349, MN876413, MN876750 MN876751, MN876538 MN876539; U.S.A., Arizona, Cochise, *T.-T.Kao 17-010*, DUKE, DB#13424, MN876609, MN875981, MN876480, MN876689, MN876270 MN876271, MN876350 MN876351, MN876414, MN876752 MN876753, MN876540 MN876541; U.S.A., Arizona, Santa Cruz, *C.J.Rothfels 2537*, DUKE, DB#5422, MN876599, MN875971, MN876470, MN876679, MN876254 MN876255, MN876338 MN876339, MN876401, MN876738 MN876739, MN876528 MN876529; U.S.A., New Mexico, Otero, *C.J.Rothfels 2501*, DUKE, DB#5374, MN876598, MN875970, MN876469, MN876678, MN876252 MN876253, MN876336 MN876337, MN876400, MN876736 MN876737, MN876526 MN876527; ***Notholaena standleyi*** Maxon [Yellow-Green]: Mexico, Coahuila, Cuatro Cinegas, *J.Henrickson 7943b*, TEX/LL, DB#13460, MN876633, NA, NA, NA, NA, NA, NA, NA, NA; Mexico, Coahuila, Cuatro Cinegas, *J.B.Walker s.n.*, MEXU, DB#13473, MN876638, MN875995, MN876494, MN876703, MN876289 MN876290, NA, MN876433, MN876768 MN876769, MN876557 MN876558; Mexico, Coahuila, Cuatrocienegas, *J.A.Villarreal 3180*, TEX/LL, DB#13450, MN876627, NA, NA, NA, NA, NA, NA, NA, NA; Mexico, Coahuila, Francisco I. Madero, *J.Henrickson 13716*, TEX/LL,

DB#13448, MN876626, MN875992, MN876491, MN876700, NA, NA, NA, NA, NA; Mexico, Coahuila, General Cepeda, *D.Castillo 1091*, ASU, DB#13649, MN876658, MN876003, MN876502, MN876711, MN876301 MN876302, MN876373 MN876374, MN876442, MN876781 MN876782, MN876570 MN876571; Mexico, Coahuila, Parras, *G.B.Hinton 28435*, TEX/LL, DB#13457, MN876631, MN875993, MN876492, MN876701, MN876286 MN876287, MN876364, MN876430, MN876765 MN876766, MN876554 MN876555; Mexico, Durango, Cuencame, *F.Chiang 8297B*, TEX/LL, DB#13458, MN876632, NA, NA, NA, NA, NA, NA, NA, NA; Mexico, Zacatecas, Mazapil, *M.C.Johnston 10467F*, TEX/LL, DB#13432, MN876617, MN875989, MN876488, MN876697, NA, NA, NA, NA, NA; U.S.A., Texas, Brewster, *M.D.Windham 94-161*, DUKE, DB#4502, EU268708, NA, NA, NA, MK632476 MK632477, MK632600 MK632601, MK632688 MK632689, NA, NA; U.S.A., Texas, Brewster, *J.Fenstermacher 867*, SRSC, DB#13437, MN876620, MN875991, MN876490, MN876699, MN876284 MN876285, MN876363, MN876429, MN876763 MN876764, MN876552 MN876553; U.S.A., Texas, Brewster, *J.Fenstermacher 1007A*, SRSC, DB#13438, MN876621, NA, NA, NA, NA, NA, NA, NA, NA; ***Notholaena standleyi*** Maxon [Yellow]: Mexico, Chihuahua, Aldama, *J.Henrickson 18472a*, TEX/LL, DB#13655, MN876663, NA, NA, NA, NA, NA, NA, NA, NA; Mexico, Chihuahua, Batopilas, *B.L.Everitt s.n.,* ARIZ, DB#13644, MN876654, NA, NA, NA, NA, NA, NA, NA, NA; Mexico, Chihuahua, Batopilas, *R.A.Bye 10058*, MEXU, DB#13652, MN876661, NA, NA, NA, NA, NA, NA, NA, NA; Mexico, Chihuahua, Chihuahua, *T.-T.Kao 17-025*, DUKE, DB#13415, MN876603, MN875975, MN876474, MN876683, MN876260 MN876261, MN876343 MN876344, MN876405, MN876743 MN876744, MN876533; Mexico, Chihuahua, Galeana, *T.Reeves 4850*, ASU, DB#13650, MN876659, MN876004, MN876503, MN876712, MN876303 MN876304, MN876375, MN876443 MN876444, MN876783, MN876572; Mexico, Chihuahua, Ignacio Zaragoza, *M.H.Mayfield 157*, TEX/LL, DB#13656, MN876664, MN876007, MN876506, MN876715, MN876306 MN876307, MN876378, MN876446 MN876447, MN876787, MN876575; Mexico, Durango, Rodeo, *L.McGill 9340*, ASU, DB#13648, MN876657, NA, NA, NA, NA, NA, NA, NA, NA; Mexico, Sonora, Huasabas, *T.Reeves 6387*, ASU, DB#13651, MN876660, MN876005, MN876504, MN876713, NA, NA, NA, MN876784 MN876785, MN876573; U.S.A., Arizona, Cochise, *B.D.Parfitt 4357*, ASU, DB#13654, MN876662, MN876006, MN876505, MN876714, MN876305, MN876376 MN876377, MN876445, MN876786, MN876574; U.S.A., Arizona, Graham, *T.-T.Kao 17-011-6*, DUKE, DB#13508, MN876653, NA, NA, NA, NA, NA, NA, NA, NA; U.S.A., Arizona, Greenlee, *T.-T.Kao 17-013*, DUKE, DB#13425, MN876610, MN875982, MN876481, MN876690, MN876272 MN876273, MN876352 MN876353, MN876415, MN876754, MN876542; U.S.A., Colorado, Las Animas, *J.Beck 1023*, DUKE, DB#5639, MN876600, MN875972, MN876471, MN876680, MN876256, MN876340, MN876402, MN876740, MN876530; U.S.A., New Mexico, Dona Ana, *T.-T.Kao 17-016*, DUKE, DB#13427, MN876612, MN875984, MN876483, MN876692, MN876276, MN876355, MN876418 MN876419, MN876756, MN876544; U.S.A., New Mexico, Grant, *T.-T.Kao 17-014*, DUKE, DB#13426, MN876611, MN875983, MN876482, MN876691, MN876274 MN876275, MN876354, MN876416 MN876417, MN876755, MN876543; U.S.A., New Mexico, Hidalgo, *J.Metzgar 129*, DUKE, DB#3783, EU268706, NA, NA, NA, MK632478, MK632602, MK632690, NA, NA; U.S.A., New Mexico, Lincoln, *T.-T.Kao 17-017*, DUKE, DB#13428, MN876613, MN875985, MN876484, MN876693, MN876277 MN876278, MN876356 MN876357, MN876420 MN876421, MN876757, MN876545; U.S.A., New Mexico, Luna, *T.-T.Kao 17-015*, DUKE, DB#13431, MN876616, MN875988, MN876487, MN876696, MN876282, MN876360, MN876425 MN876426, MN876761, MN876549 MN876550; U.S.A., New Mexico, San Miguel, *M.Schiebout 4838*, UNM, DB#13463, MN876634, MN875994, MN876493, MN876702, MN876288, MN876365, MN876431 MN876432, MN876767, MN876556; U.S.A., New Mexico, San Miguel, *B.Reif 9383*, UNM, DB#13464, MN876635, NA, NA, NA, NA, NA, NA, NA, NA; U.S.A., New Mexico, Sandoval, *B.Jacobs 4318*, UNM, DB#13465, MN876636, NA, NA, NA, NA, NA, NA, NA, NA; U.S.A., New Mexico, Sierra, *C.J.Rothfels 2513*, DUKE, DB#5389, MK632843, NA, NA, NA, MK632479 MK632480, MK632603, MK632691, NA, NA; U.S.A., New Mexico, Socorro, *T.-T.Kao 17-018*, DUKE, DB#13429, MN876614, MN875986, MN876485, MN876694, MN876279 MN876280, MN876358, MN876422, MN876758, MN876546; U.S.A., Oklahoma, Cimarron, *J.Beck 1025*, DUKE, DB#5641, MN876601, MN875973, MN876472, MN876681, MN876257 MN876258, MN876341, MN876403, MN876741, MN876531; U.S.A., Oklahoma, Greer, *T.-T.Kao 17-001*, DUKE, DB#13416, MN876604, MN875976, MN876475, MN876684, MN876262, MN876345, MN876406 MN876407, MN876745, MN876534; U.S.A., Texas, Brewster, *M.D.Windham 94-160*, DUKE, DB#4549, MN876593, MN875968, MN876467, MN876676, MN876250, MN876334, MN876396 MN876397, MN876733, MN876524; U.S.A., Texas, Brewster, *A.M.Powell 6106*, SRSC, DB#13441, MN876623, NA, NA, NA, NA, NA, NA, NA, NA; U.S.A., Texas, Hudspeth, *M.D.Windham 94-162*, DUKE, DB#5096, MN876596, MN875969, MN876468, MN876677, MN876251, MN876335, MN876398 MN876399, MN876734 MN876735, MN876525; U.S.A., Texas, Hudspeth, *J.Fenstermacher s.n.,* SRSC, DB#13443, MN876625, NA, NA, NA, NA, NA, NA, NA, NA; U.S.A., Texas, Hudspeth, *A.Treuer-Kuehn V-0832.2*, TEX, DB#13453, MN876630, NA, NA, NA, NA, NA, NA, NA, NA; U.S.A., Texas, Jeff Davis, *C.J.Rothfels 2489*, DUKE, DB#5363, MN876597, NA, NA, NA, NA, NA, NA, NA, NA; U.S.A., Texas, Jeff Davis, *J.Beck 1046*, DUKE, DB#5662, MN876602, MN875974, MN876473, MN876682, MN876259, MN876342, MN876404, MN876742, MN876532; U.S.A., Texas, Jeff Davis, *S.C.Yarborough 2002-7*, SRSC, DB#13442, MN876624, NA, NA, NA, NA, NA, NA, NA, NA; U.S.A., Texas, Presidio, *M.K.Terry 908*, SRSC, DB#13435, MN876618, MN875990, MN876489, MN876698, MN876283, MN876361 MN876362, MN876427 MN876428, MN876762, MN876551; U.S.A., Texas, Presidio, *E.J.Lott 5070*, SRSC, DB#13436, MN876619, NA, NA, NA, NA, NA, NA, NA, NA; U.S.A., Texas, Presidio, *W.R.Carr 20007*, TEX, DB#13451, MN876628, NA, NA, NA, NA, NA, NA, NA, NA; U.S.A., Texas, Presidio, *E.J.Lott 5070*, TEX, DB#13452, MN876629, NA, NA, NA, NA, NA, NA, NA, NA; U.S.A., Texas, Terrell, *P.Zelazny 195*, SRSC, DB#13440, MN876622, NA, NA, NA, NA, NA, NA, NA, NA.

Outgroup: ***Aleuritopteris argentea*** (S.G. Gmel.) Fée, Cultivation, NA, NA, *T.-T.Kao 19-001*, DUKE, DB#13908, MN876666, MN876009, MN876508, MN876717, MN876309 MN876310, NA, MN876448 MN876449, MN876790 MN876791, MN876577; ***Cheilanthes leucopoda*** Link, Mexico, Tamaulipas, NA, *Gastony 90-10-4A*, IND, DB#5075, MN876667, MN876010, MN876509, MN876718, MN876311 MN876312, MN876380, MN876450, MN876792, MN876578; ***Cheilanthes pruinata*** Kaulf., Cultivation, NA, NA, *H.Forbes s.n.,* UC, DB#9564, MK632818, MN876011, MN876510, MN876719, MN876313 MN876314, MN876381, MN876451, MN876793, MN876579; ***Cheiloplecton rigidum*** (Sw.) Fée var. ***rigidum***, Mexico, Colima, Ixtlahuacan, *C.J.Rothfels 3203*, DUKE, DB#6617, JQ855904, MN876012, MN876511, MN876720, MN876315 MN876316, MN876382, MN876452, MN876794, MN876580; ***Gaga hintoniorum*** (M.G.Mendenh. & G.L.Nesom) F.W.Li & Windham, Mexico, Nuevo León, Rayones, *H.F.Olvera 1805*, DUKE, DB#13907, NA, NA, NA, NA, NA, MN876383, NA, NA, MN876581; ***Gaga hirsuta*** (Link) F.W. Li & Windham, Costa Rica, San José, Acosta, *C.J.Rothfels 08-023*, DUKE, DB#5133, JX313492, MN876013, MN876512, MN876721, MN876317, NA, MN876453 MN876454, MN876795, NA; ***Myriopteris aurea*** (Poir.) Grusz & Windham, Cultivation, NA, NA, *T.-T.Kao 19-002*, DUKE, DB#13910, MN876668, MN876014, MN876513, MN876722, MN876318 MN876319 MN876320, MN876384 MN876385, MN876455, MN876796, MN876582; ***Notholaena aschenborniana*** Klotzsch, U.S.A., Arizona, Cochise, *E.Schuettpelz 476*, DUKE, DB#3183, MN876669, MN876015, MN876514, MN876723, MN876321 MN876322, MN876386, MN876456 MN876457, MN876797 MN876798, MN876583; ***Notholaena aureolina*** Yatskievych & Arbelaez, Costa Rica, Guanacaste, Santa Cruz, *C.J.Rothfels 08-049*, DUKE, DB#5139, MK632826, MN876016, MN876515, MN876724, MN876323, MN876387, MN876458, MN876799, MN876584; ***Notholaena brachypus*** (Kunze) J. Sm., Mexico, Jalisco, NA, *G.Yatskievych 89-236*, IND, DB#4517, MN876670, MN876017, MN876516, MN876725, MN876324 MN876325, MN876388 MN876389, MN876459, MN876800, MN876585; ***Notholaena bryopoda*** Maxon, Mexico, Nuevo León, General Zaragoza, *H.F.Olvera 1745*, DUKE, DB#13909, MN876671, MN876018, MN876517, MN876726, MN876326, MN876390, MN876460, MN876801, MN876586; ***Notholaena grayi*** Davenp., U.S.A., Arizona, Pima, *T.-T.Kao 17-007*, DUKE, DB#13421, MN876672, MN876019, MN876518, MN876727, MN876327 MN876328,

MN876391, MN876461, MN876802, MN876587; ***Notholaena lemmonii*** **D.C. Eaton**, Mexico, Guerrero, Zirndaro, *Campos 932*, MEXU, DB#7087, MK632836, MN876020, MN876519, MN876728, MN876329, MN876392, MN876462, MN876803, MN876588; ***Notholaena sulphurea*** **(Cav.) J. Sm [chemotype Cream]**, Mexico, San Luis Potosi, Villa Juarez, *H.F.Olvera 1730A*, DUKE, DB#13462, NA, MN876021, MN876520, MN876729, MN876330, MN876393, MN876463, MN876804 MN876805, MN876589; ***Paragymnopteris marantae*** **(L.) R.M. Tryon**, China, Yunnan, Jianchuan, *G.Yatskievych Feb-35*, KUN, DB#3736, MN876673, MN876022, MN876521, MN876730, MN876331, MN876394, MN876464, MN876806, MN876590; ***Pentagramma pallida*** **(Weath.) Yatsk. Windham & E. Wollenw.**, U.S.A., California, Kern, *M.D.Windham 3433*, DUKE, DB#3842, MN876674, MN876023, MN876522, MN876731, MN876332, MN876395, MN876465, MN876807, NA.